1. Introduction

Several earlier reports[1-3] have documented the history of the design of beam lines 2A. Reference 1 details the design in which the experimental building of the Isotope Separator and ACcelerator (ISAC) complex perpendicular to the cyclotron building of TRIUMF. In this design, three positions were allotted for target locations. Subsequently, the ISAC complex was rotated such that it became parallel to the cyclotron building with the number of target locations reduced to two. This is the subject of references 2 and 3, the latter proposing a modification of the former.

For reasons discussed below, recalculation of the optics of the beam line was required. This report presents the results of the recalculation. Because beam line components are being installed according to the dictates of this recalculation, the results reported here should be considered as the final design of the beam line.

2. Differences between this and previous optics calculations for beam line 2A

Since references 2 and 3 were issued three things have arisen that have made it necessary to recompute the beam line optics. We list these below.

1. On completion of the ISAC complex it was found that the ISAC complex and the accelerator building were out of parallel by $2' 7''$. The use of two targets is predicated on them being orientated symmetrically about a line perpendicular to the south wall of the building so that either target could feed beam to the mass spectrometer. Consequently, it was necessary to take up the degree of non-parallelism in beam line 2A.

2. During 1997 the quadrupoles and dipoles required for the beam line were delivered to TRIUMF. These were field mapped and their effective lengths were measured. Previous optics calculations had been made with generic effective lengths; with measured effective lengths now available these calculations could now be redone.

3. In preparing to redo the optics calculations it was noted that the extraction parameters (fringe-field matrices) that had been used showed some unusual oscillations. A request was made of R. Lee to review the calculation of these parameters with a view to removing these oscillations. Recalculation of the fringe field parameters was completed in December, 1997[4].

3. Design modification

Figure 1 shows the present configuration of beam line 2A. Shown are the beam delivery systems to each of the east and west targets, labelled TGT1 and TGT2 respectively. Only the latter will be installed initially. In this figure and throughout this report, element locations are specified in a Cartesian coordinate system that is located with its origin $(x_0, y_0) = (0, 0)$ at the cyclotron center. The positive x-axis is directed east and the positive y-axis is directed north.

As a consequence of the non-parallelism of the cyclotron and ISAC buildings, the vault dipoles 2AVB1 and 2AVB2 that in previous designs each deflected the beam 27.5° are now required to deflect the beam 27.471° and 27.564° respectively. In addition, the cross-over point of 2AVB2 was moved upstream by approximately 2 in. Additional corrections were made in some element separations and in that of the two 15° dipoles 2AB3 and 2AB4, although their bend angles were left unchanged.

Extraction studies track the stripped beam from the stripper foil to a point well beyond the (effective) edge of the combination magnet. Consequently, it is necessary to determine that location in order to specify the location of the components of the beam line. For completeness we include the following section from ref[3].

3.1 Starting Point of the Beam line

(Data in this section from the the calculation of the previous (oscillating) fringe-field parameters[5]. However, in their recalculation *only* the extraction parameters change because the extracted beam is constrained to exit the cyclotron at a given point and at a given angle. Consequently, previous calculations of the starting point of the beam line are valid.)

The upper portion of figure 2 shows the trajectories of the extracted beam as calculated by R Lee; the lower portion shows the essential geometry of extraction. It is seen that the crossover point of the combination magnet is located at an (R, θ) coordinate of (412.32 inches, 327.00°) with respect to the centerline of valley 3. Consequently, the radius vector makes an angle of $(29° + 327° - 360°) = -4.0°$ with respect to the positive x-axis of this report. In this coordinate system then, the crossover point is located at the coordinates

$$\begin{aligned}(x_{co},\, y_{co}) &= (412.32\cos(-4.0°),\ 412.32\sin(-4.0°)) \text{ inches} \\ &= (411.315609,\ -28.761989) \text{ inches} \\ &= (10.447417,\ -0.730555) \text{ m.}\end{aligned}$$

Because the effective length of the combination magnet has been taken as 13.78 inches (0.35 m) and assuming that the crossover point is at the center of the magnet, we then calculate the distance from there to the magnet edge as

$$\begin{aligned}(\delta x,\, \delta y) &= (6.89\cos(35.0°), 6.89\sin(35.0°)) \text{ inches} \\ &= (5.643958,\ 3.951942) \text{ inches} \\ &= (0.143357,\ 0.100379) \text{ m.}\end{aligned}$$

Thus the exit edge of the magnet is located at

$$\begin{aligned}x_{magexit} &= x_{co} + \delta x \\ &= (10.447417 + 0.143357) \text{ m} \\ &= 10.590774 \text{ m}\end{aligned}$$

and

$$\begin{aligned}y_{magexit} &= y_{co} + \delta y \\ &= (-0.730555 + 0.100379) \text{ m} \\ &= -0.630176 \text{ m.}\end{aligned}$$

From ref[5] we find that at 489.466 MeV the tracing done to generate the fringe-field transfer matrices ends at $(R_{traj}, \theta_{traj}) = (436.345 \text{ inches}, 329.511°)$. Thus, in the (x, y) system used here, the extracted trajectory makes an angle with respect to the positive x-axis of $(29° + 329.511° - 360°) = -1.489°$ and the end of the fringe-field calculation becomes

$$\begin{aligned}(x_{traj},\, y_{traj}) &= (436.345\cos(-1.489°),\ 436.345\sin(-1.489°)) \text{ inches} \\ &= (436.197660,\ -11.338437) \text{ inches} \\ &= (11.079421,\ -0.287996) \text{ m.}\end{aligned}$$

Thus we must back up a distance

$$\begin{aligned}\Delta_{490} &= \sqrt{(x_{traj} - x_{magexit})^2 + (y_{traj} - y_{magexit})^2} \\ &= \sqrt{(11.079421 - 10.590774)^2 + (-0.287996 - (-0.630176))^2} \\ &= \sqrt{(0.488647)^2 + (0.342180)^2} \\ &= 0.596543 \text{ m}\end{aligned}$$

along the exiting trajectory to reach the magnet exit. Similar calculations at an energy of 499.456 MeV [end-point $(R_{traj}, \theta_{traj}) = (436.169 \text{ in.}, 329.493°)$] and 479.477 MeV [end-point $(R_{traj}, \theta_{traj}) = (436.498 \text{ in.}, 329.526°)$] yield values of $\Delta_{500} = 0.590696$ m and $\Delta_{480} = 0.601392$ m respectively. We average these to obtain the average back-up distance

$$\Delta_{av} = 0.59621 \text{ m}.$$

In the TRANSPORT calculations presented here, a back-up distance of 0.59617 m was used (in error). However, the 0.4 mm error introduced will have no effect on the calculations.

4. Revised extraction data

Details of the recalculated extraction parameters together with measured combination magnet data are given in ref[6]. For completeness we give here excerpts of that report.

The revised extraction parameters of ref[4] for beam line 2A cover an energy range from 470 MeV to 510 MeV. Table 1 lists the stripping radius and angle and the combination magnet field that were obtained in these calculations. The rightmost column of the table gives an estimate of the current required to produce the calculated field. Table 2 lists the revised transfer matrix elements in units suitable for use in the program TRANSPORT[7]. As an indication of the difference between the previous and recalculated values, figures 3 and 4 show the values of R_{11} and R_{12}, respectively, of the recalculated and original parameters over the energy range of extraction. Recalculated values are shown as diamonds and the original values are plotted as a dotted line. The oscillations of the previous extraction parameters are readily apparent. In particular, the values of R_{11} have a peak-to-peak variation of approximately a factor of five. Those of R_{12} have a peak-to-peak variation of approximately 1%. The values of the recalculated parameters are seen to lie on a (relatively) smooth line.

Similar plots for R_{21} and R_{22} are shown in figures 5 and 6 where again oscillations are apparent in the original parameters with a peak-to-peak variation of R_{21} and R_{22} of approximately 1.5% and 2% respectively. The recalculated parameters are seen to lie on relatively smooth curves.

The dispersion parameters R_{16} and R_{26} do not differ significantly between the two calculations, nor do the vertical parameters R_{33}, R_{34}, R_{43} and R_{44}. These are not shown.

5. Beam Line Design

5.1 General Considerations

Other than transport element settings, there has been no change in the beam optics of the beam line. The design philosophy of ref[2,3] has been maintained. Again, for completeness, we summarize the optics of the beam.

In the cyclotron vault, a quadrupole doublet located downstream of the combination magnet and upstream of the first of two 27.5° dipoles and a second doublet positioned downstream of the second dipole are used to control the vertical beam height in the dipoles and to produce a horizontal waist at the point labelled WST1 in figure 1. A vertical waist is located approximately 0.9 m upstream of the horizontal waist. This split-waist design arose from the REVMOC[8] calculations that are discussed below. In addition, a beam size of $(\pm x, \pm y) = (\pm 1.1, \pm 0.66)$ cm is required at the horizontal waist location.

The first doublet is composed of two of the standard TRIUMF 4Q14/8 quadrupoles. Those of the second doublet are of a new TRIUMF design [8,9], modified as suggested by A. Otter [10], and are akin to the TRIUMF 4Q9/8 quadrupoles that were purchased from Alpha Magnetics some time ago. These new quadrupoles are designated as TRIUMF type 4Q8.5/8.

The section of beam line from the WST1 to the WST3 locations carries the beam through the vault wall and into the 2A tunnel. It consists of the triplet 2AVQ5/6/7 of 4Q8.5/8.5 quadrupoles just inside the north wall of the vault followed by the 2AQ8/9/10 triplet of 4Q14/8 quadrupoles. The first triplet produces a double waist at the position labelled WST2, approximately 8 m from the external wall of the vault. The second triplet produces another double waist at the location labelled WST3. These two triplets are tuned to keep the vertical size of the beam small and to produce a vertical beam size of ± 0.29 cm at WST3.

The section of beam line between the WST3 and WST4 locations is composed of the quadrupole doublet 2AQ11/12. These quadrupoles, of the 4Q6.5/8.5 type, are used to produce another double waist at the WST4 location.

5.2 The WST4 to target sections

The section of beam line that feeds the west target (labelled TGT2 in figure 1) consists of the two quadrupole doublets 2AQ13/14 and 2AQ15/16, and two 15° rectangular dipole magnets 2AB3 and 2AB4; all of these quadrupoles are of the 4Q8.5/8.5 variety. These quadrupoles are used to produce a nominal beam size at west target location of ± 2 mm in each of the horizontal and vertical planes and, at the same time, to produce a spatially achromatic beam spot ($R_{16} = 0$, $R_{26} \neq 0$) at the target.

When the east target (labelled TGT1 in figure 1) is installed, the 2AB3 15° dipole will be moved to a location opposite 2AB4, a $\pm 15°$ switching magnet will be installed at the present location of 2AB3 and a quadrupole doublet, 2AQ17/18, of the 4Q8.5/8.5 type will be added to produce the symmetric system shown in figure 1.

A TRANSPORT listing for delivery of a 500 MeV beam to the west target (TGT2) is given in table 2. Figure 7 shows the beam envelopes along the beam line for beam delivery to that target. Note that the horizontal half-width of the beam is plotted as positive whereas the vertical half-width is plotted as negative. The 'tail' that appears in this plot at the beginning of the beam line is a result because of the back-up that is required to the effective exit of the combination magnet. We again note that in this and all succeeding figures the cyclotron center is taken as $(x, y) = (0,0)$.

TRANSPORT calculations for energies of 480, 489, 490, 491 and 492 MeV have also been made. Their beam profiles do not differ significantly from those at 500 MeV and, consequently, are not shown.

Table 3 is a TRANSPORT listing for delivery of a 500 MeV beam to the east target (TGT1). Element settings upstream of WST4 are identical to those for beam delivery to the west target; only the settings of quadrupoles 2AQ13/14 and 2AQ17/18 change. Of course, the directions of bend of the two 15° dipoles are reversed. Figure 8 shows the beam envelopes for this case.

An expanded view of the beam profiles in the vault section section of the beam line is shown in figure 9. Figure 10 is a similar plot of the beam profiles through the long drift from the vault to the WST3 location in the 2A tunnel. Beam profiles between the WST3 and WST4 locations are shown in figure 11. As noted above, because the settings of the transport elements are identical upstream of WST4, these profiles will be the same *regardless* of which target is being fed beam.

Figure 12 shows the beam profiles from WST4 to the west target and figure 13 shows those to the east target. The profiles in this section of beam line differ because the beam line is *not* achromatic and the 15° dipoles bend in opposite directions when directing beam to the east and west targets. This is the reason that the element settings differ in the two cases.

5.3 Settings of the beam-transport elements

Table 4 lists the settings of the various elements of the transport system for energies of 480, 489, 490, 491, 492 and 500 MeV. Because element settings upstream of WST4 are the same for operation of either target, we list in table 4 only the settings for 2AQ13/14 and 2AQ17/18 that are required for beam delivery to the east target.

Table 5 lists the calculated beam sizes at the various waist locations.

Beam sizes and overall transfer matrices at the west target location are listed in table 6; those at the east target location are listed in table 7.

6. REVMOC calculations

The program REVMOC was run at energies of 480, 490, 491, 492 and 500 MeV to estimate the amount of beam spill to be expected and where such might occur. REVMOC is a Monte Carlo program that traces particles through a beam optics configuration using true second-order optics, although the effects of chromatic aberrations is considered to all orders. The effects of multiple scattering, decay, nuclear scattering and energy loss in scatterers, absorbers, collimators, slits and apertures are included. Geometric effects are considered locally to only second order but higher-order global effects will appear because of the accumulation of the second-order effects. The program does not, however, optimize beam elements and its primary use is to do detailed checks on a beam line that has been designed using the program TRANSPORT.

For each energy and each target configuration 150,000 particles were traced through the beam line. Except in one instance a spill no greater than 0.0094% of the beam was recorded and that loss was predicted to occur between the stripper foil and the combination magnet exit. In the one case that predicted a larger spill—480 MeV at TGT1—an additional spill of 0.0013% was predicted to occur near the entrance of the 2A tunnel. This is considered an anomaly because no spill was predicted there with the beam line tuned for delivery to TGT2 and the tune of the beam line upstream of WST4 was unchanged.

Figure 14 is a plot of the vertical divergence (DY) in mr along the vertical axis versus the vertical beam size (Y) in cm along the horizontal axis at the WST1 location. The upper portion of the plot is a prediction of this correlation *without* any foil scattering taken into account; the lower portion is the prediction taking into account the scattering in a carbon stripper foil that is 0.00003 m (0.0012 in.) thick. It is clear that the foil scattering adds significantly to the (vertical beam divergence. The reason for this is the extremely small vertical divergence of the beam at the point of stripping.

Predicted beam sizes along the line do not differ significantly as a function of energy. For this reason we show only profiles predicted for a 500 MeV beam. Figure 15 shows the predicted beam spot at the WST1 target location for a beam energy of 500 MeV. The spot size shown includes the effect of foil scattering. The units of the vertical and horizontal scales are cm. Figures 16 through 18 are similar plots at the WST2, WST3 and WST4 locations respectively.

Figures 19 and 20 are similar plots of the beam profiles at the TGT2 (west target) and TGT1 (east target) locations respectively.

Using the data presented in figure 19, we find that REVMOC predicts that at the west target 0.03% (2.18%) of the beam lies *outside* the nominal design spot size of ± 0.22 cm in the horizontal (vertical) plane at a beam energy of 500 MeV. From figure 20 we see that 0.87% (2.03%) of the beam lies outside of these nominal dimensions.

At 490 MeV we find the corresponding values of percentages of beam outside the nominal design values are 0.05% (2.05%) for the horizontal (vertical) plane at TGT2 and 0.19% (2.36%) for the horizontal (vertical)

plane at TGT1. At 480 MeV the corresponding percentages of beam outside of the nominal design values are 0.09% (2.00%) for the horizontal (vertical) plane at TGT2 and 1.00% (2.53%) for the horizontal (vertical) plane at TGT1.

Assuming that the vertical and horizontal beam losses are independent, we may then calculate the probability of beam lying outside of an area ±0.22 cm square. Thus at 500 MeV and for beam delivery to the west target (TGT2), we have

$$\begin{aligned} \mathrm{P}(x > \pm 0.22 \text{ cm and } y > \pm 0.22 \text{ cm}) &= \mathrm{P}(x > \pm 0.22 \text{ cm}) + \mathrm{P}(y > \pm 0.22 \text{ cm}) \\ &\quad - \mathrm{P}(x > \pm 0.22 \text{ cm}) \times \mathrm{P}(y > \pm 0.22 \text{ cm}) \\ &= 0.0003 + 0.0218 - (0.0003)(0.0218) \\ &= 0.0221 \end{aligned}$$

and for delivery to the east target (TGT1) we have

$$\begin{aligned} \mathrm{P}(x > \pm 0.22 \text{ cm and } y > \pm 0.22 \text{ cm}) &= \mathrm{P}(x > \pm 0.22 \text{ cm}) + \mathrm{P}(y > \pm 0.22 \text{ cm}) \\ &\quad - \mathrm{P}(x > \pm 0.22 \text{ cm}) \times \mathrm{P}(y > \pm 0.22 \text{ cm}) \\ &= 0.0087 + 0.0203 - (0.0087)(0.0203) \\ &= 0.0288. \end{aligned}$$

Thus, at 500 MeV, approximately 97% of the beam is predicted to lie within an area ±0.22 cm square at either target. Because the basic data is similar results for other energies, we may assume that this result applies across the energy region.

Finally, figure 21 shows a plot of momentum p in GeV/c along the vertical axis versus horizontal position x in cm along the horizontal axis at the TGT2 location. That momentum and horizontal position are uncorrelated indicates that the beam is spatially achromatic there. Similar plots for the other energies show the same property.

7. The effect of windows at the end of the beam line

The beam line will not be operated with the stripper foil as the only scattering element. An aluminum widow with a thickness of 0.005 inch will be installed approximately 44 inches (1.118 m) upstream of the target in order to isolate beam line and cyclotron vacuum systems from the relatively poor and possibly dirty vacuum of the target enclosure. In addition, a copper window 0.010 inch thick is located 16 inches upstream of the target at the entrance of the target vessel. Consequently, REVMOC runs were made to find the effect of these windows on the beam spot at the target itself.

Figure 22 shows the result of such a run and shows the effects of the stripper foil and of the aluminum and copper windows. This figure is to be compared with figure 19 that shows the effect of the stripper foil only. Runs were made only at 500 MeV and for the west (TGT2) location on the assumption that similar effects would be observed at the other energies and at the east (TGT1) location.

Figure 22 shows that the effect of the additional windows is to increase significantly the percentage of beam outside of the design goal of ±2 mm in each plane. In fact, the figure shows that scattered beam covers the entire 10 cm diameter of the beam pipe. However, it also shows that most of the beam lies within ±0.52 cm. Figure 23 shows the same data plotted over smaller scales. Here 99.6% of the beam is shown to lie within ±0.51 cm in each of the horizontal planes. On the other hand, only 88.1% of the beam in the horizontal plane and 84.4% in the vertical plane lie within the nominal design values of ±0.21 cm. However, the vertical and horizontal beam profiles are much more similar and one could argue that, in a sense, the introduction of the windows symmetrizes the beam at the expense of doubling the beam size in each of the horizontal and vertical planes.

8. Current settings for various energies

This section contains estimates for the power supply settings for the various beam line elements as a function of energy. Data given here has already been passed to the Cyclotron Operations Group and is included here for completeness.

During 1997 dipole, quadrupole and steering magnets were field mapped as they arrived. This data was analysed with the program PLOTDATA [9] to produce analytic fits to the $B-I$ data. These were then inverted and used to estimate the current required to set the transport elements to their appropriate values.

8.1 Combination magnet settings

The currents for the combination magnet that are listed in table 1 were obtained by first fitting the calculated combination magnet field and energy data with PLOTDATA. This gave the relationship [6]

$$B = 1153.09 - 678.6901\left[\frac{E}{100}\right] + 135.9815\left[\frac{E}{100}\right]^2 - 9.283356\left[\frac{E}{100}\right]^3$$

with B in kG and E in MeV. The measured $B-I$ data covered a region from 0 to 9.15 kG corresponding to currents from 0 to 500 A. Because the energy range of extraction is between 470 MeV and 510 MeV the 'useful' range of combination magnet fields lies between ± 4 kG. The data was then fitted over this region to give more accurate predictions of the fields in the energy range of interest. The resulting expression for the $B-I$ relationship was

$$B = -0.1340001 + 2.305834\left[\frac{I}{100}\right] - 0.29800038\left[\frac{I}{100}\right]^2 + 0.07666675\left[\frac{I}{100}\right]^3$$

with B in kG and I in Amperes and the inverse $I-B$ relationship

$$I = 100\,[0.06990472 + 0.415772\,B + 0.0422539\,B^2 - 0.005627461\,B^3]$$

again with I in Amperes and B in kG.

8.2 Vault dipole magnet settings

Field measurements of the two 27.5° vault dipoles were virtually identical. From the measured $B-I$ data over the useful field region from 12.9 to 15.8 kG (corresponding to currents from 500 to 650 Amperes) the relationship between the field and the current had the form

$$B = -2.129611 + 3.828047\left[\frac{I}{100}\right] - 0.1652398\left[\frac{I}{100}\right]^2$$

with B in kG and I in Amperes. The inverse $I-B$ relationship was

$$I = 100\,[3.007062 - 0.1411699\,B + 0.02298545\,B^2]$$

again with I in Amperes and B in kG.

8.3 Tunnel dipole magnet settings

As was the case with the vault dipoles, field measurements were virtually identical for the two 15° dipoles. Over the useful field region from 9.1 to 11.4 kG the following expression was found for the $B-I$ relationship

$$B = 6.593975 - 1.984003\left[\frac{I}{100}\right] + 0.797258\left[\frac{I}{100}\right]^2 - 0.055583\left[\frac{I}{100}\right]^3$$

with B in kG and I in Amperes together with the inverse $I-B$ relationship

$$I = 100\,[-6.129738 + 2.40779\,B - 0.1974853\,B^2 + 0.006989399\,B^3]$$

again with I in Amperes and B in kG.

8.4 Quadrupole type 4Q8.5/8.5 magnet settings

Only one quadrupole of this type was completely field-mapped although the effective lengths of each quadrupole of this type was measured. From the measured $B-I$ data for this type of quadrupole the following relationship was found

$$B = -0.3355125 + 4.366226\left[\frac{I}{100}\right] - 2.176171\left[\frac{I}{100}\right]^2 + 1.442828\left[\frac{I}{100}\right]^3 - 0.4386762\left[\frac{I}{100}\right]^3 + 0.04577269\left[\frac{I}{100}\right]^3$$

with B in kG and I in Amperes. The inverse $I-B$ relationship was

$$I = 100\,[\,-0.07974771 + 0.4830017\,B - 0.09224173\,B^2 + 0.02866291\,B^3 - 0.004150654/,B^4 + 0.0002334605\,B^5\,]$$

again with I in Amperes and B in kG.

8.5 Quadrupole type 4Q14/8 magnet settings

Full $B-I$ curves were taken for quadrupoles 2AVQ1 and 2AVQ2. Each of these displayed a slightly different field-current relationship. However, all quadrupoles of this type had their effective lengths measured.

For 2AVQ1 the fitted $B-I$ relationship was, with B in kG and I in Amperes,

$$B = -0.0249549 + 1.838984\left[\frac{I}{100}\right] - 0.03859897\left[\frac{I}{100}\right]^2$$

with its inverse $I-B$ relationship

$$I = 100\,[0.004643126 + 0.5423253\,B + 0.002235214\,B^2\,]$$

For 2AVQ2 the fitted $B-I$ relationship was, with B in kG and I in Amperes,

$$B = -0.02154864 + 1.84451\left[\frac{I}{100}\right] - 0.0259896\left[\frac{I}{100}\right]^2$$

with its inverse $I-B$ relationship

$$I = 100\,[0.003909051 + 0.5409259\,B + 0.001523562\,B^2\,]$$

8.6 Estimates of the current requirements of the transport elements

Table 8 lists the estimated currents of the transport elements for beam delivery to the west (TGT2 target for the energies considered in this report. Because $B-I$ curves for the 4Q14/8 type quadrupoles 2AQ8/9/10 were not made, an estimate based on each of quadrupole 2AVQ1 and 2AVQ2 is given in the tabulation.

9. Discussion

Since a proposal for an ISAC facility was first made, many versions of its beam transport line have been considered. This report presents the final configuration of the beam line as it it presently being installed.

Revised extraction matrices have been produced for energies from 470 to 500 MeV and beam-line optics for some of these energies have been developed. In addition, beam spill calculations were made. These indicated that beam spill should be contained within the cyclotron vault.

It should be noted, however, that the accuracy to which the program REVMOC was asked to predict beam spill is, at best, at the limit of the program. In normal use, one would expect an accuracy of 0.5% at best. Thus the quoted beam spills should be regarded as indications that spill might occur rather than an absolute value to be quoted.

A study of the effect of a vacuum window at the end of the beam line has been made. The results indicate that the window would increase the beam size by 2 mm in each of the horizontal and vertical planes. It is felt that this increase is reasonable and, in any event, the presence of the window is necessary. It is possible that the optics of the beam line could be modified to produce a smaller beam spot at the targets if necessary.

References

1. G. M. Stinson, *A 480 MeV to 500 MeV beamline 2A transport system to an ISAC Facility*, TRI-DNA-95-2, TRIUMF, October, 1995.

2. G. M. Stinson, *A 480 MeV to 500 MeV beam transport system to an ISAC Facility*, TRI-DNA-96-5, TRIUMF, July, 1996.

3. G. M. Stinson, *A revision of the 480 MeV to 500 MeV beam transport system to an ISAC Facility*, TRI-DNA-95-2, TRIUMF, October, 1996.

4. R. Lee, *Private communication*, TRIUMF, December 10, 1997.

5. R. Lee, *Private communication*, TRIUMF, October, 1965.

6. G. M. Stinson, *Revised extraction data for beam line 2*A, TRI-DNA-98-1, TRIUMF, January, 1998.

7. K. L. Brown, F. Rothacker, D. C. Carey and Ch. Iselin, *TRANSPORT, A Computer Program for Designing Charged Particle Beam Transport Systems*, CERN Report CERN 80-04, CERN, 1980.

8. C. Kost and P. Reeve, *REVMOC: Monte Carlo Beam Transport Program*, TRI-DN-82-28, TRIUMF, 1982.

9. J. L. Chuma, *Plotdata Command Reference Manual*, TRIUMF Report TRI-CD-87-03b, TRIUMF, June, 1991.

Table 1
Stripping radius and angle and calculated combination magnet fields and currents for beam line 2A

Energy (MeV)	Stripping coordinates		Combination magnet field (kG)	Combination magnet current (A)
	Radius (in.)	θ (°)		
470	300.137	306.413	3.24704	167.279
471	300.141	306.576	3.09329	159.377
472	300.146	306.739	2.94113	151.510
473	300.150	306.900	2.78680	143.495
474	300.154	307.060	2.63448	135.563
475	300.158	307.219	2.48425	127.729
476	300.162	307.379	2.33002	119.689
477	300.166	307.539	2.17732	111.742
478	300.170	307.696	2.02744	103.966
479	300.174	307.852	1.87581	96.136
480	300.177	308.008	1.72584	88.440
481	300.181	308.163	1.57662	80.840
482	300.185	308.317	1.42645	73.263
483	300.189	308.470	1.27745	65.826
484	300.192	308.621	1.13126	58.618
485	300.195	308.771	0.98253	51.387
486	300.199	308.922	0.83537	44.344
487	300.202	309.071	0.68998	37.505
488	300.205	309.221	0.54102	30.633
489	300.208	309.370	0.39516	24.045
490	300.211	309.520	0.24779	17.544
491	300.215	309.670	0.09830	11.118
492	300.218	309.819	−0.04883	−9.031
493	300.221	309.969	−0.19727	−15.353
494	300.224	310.118	−0.34632	−21.873
495	300.227	310.267	−0.49428	−28.506
496	300.230	310.417	−0.64355	−35.348
497	300.233	310.565	−0.79346	−42.360
498	300.237	310.715	−0.94312	−49.490
499	300.240	310.864	−1.09280	−56.738
500	300.243	311.013	−1.24456	−64.196

Table 1 (Continued)

Stripping radius and angle and calculated combination magnet fields and currents for beam line 2A

Energy (MeV)	Stripping coordinates		Combination magnet field (kG)	Combination magnet current (A)
	Radius (in.)	θ (°)		
501	300.246	311.162	−1.39349	−71.611
502	300.250	311.311	−1.54458	−79.218
503	300.252	311.463	−1.69744	−86.988
504	300.255	311.615	−1.85137	−94.878
505	300.258	311.770	−2.00631	−102.878
506	300.264	311.921	−2.16272	−110.982
507	300.268	312.074	−2.31634	−118.976
508	300.271	312.230	−2.47797	−127.402
509	300.276	312.389	−2.63902	−135.800
510	300.280	312.552	−2.80377	−144.378

Table 2
Transfer matrix elements for beam line 2A

Energy (MeV)	Horizontal transfer matrix elements					
	R_{11} (cm/cm)	R_{12} (cm/mr)	R_{16} (cm/%)	R_{21} (mr/cm)	R_{22} (mr/mr)	R_{26} (mr/%)
470	−0.01938	0.333018	1.41816	−3.05430	0.17448	2.37640
471	−0.01985	0.332567	1.41315	−3.05560	0.17392	2.37860
472	−0.01362	0.331810	1.40749	−3.04250	0.17265	2.37920
473	−0.02049	0.330994	1.40333	−3.06030	0.17122	2.38320
474	−0.02086	0.330734	1.38757	−3.06310	0.17113	2.36020
475	−0.02129	0.330275	1.39543	−3.06530	0.17068	2.39160
476	−0.02126	0.329538	1.38925	−3.06560	0.16951	2.39120
477	−0.02160	0.329436	1.37422	−3.06780	0.16985	2.37000
478	−0.02265	0.329040	1.38053	−3.07160	0.16942	2.39750
479	−0.02219	0.328514	1.37574	−3.07180	0.16876	2.39980
480	−0.02257	0.328475	1.36150	−3.07450	0.16920	2.38040
481	−0.02310	0.328181	1.36757	−3.07630	0.16917	2.40710
482	−0.02300	0.327777	1.36115	−3.07570	0.16884	2.40560
483	−0.02410	0.327828	1.34868	−3.07570	0.16958	2.38970
484	−0.02196	0.327590	1.35484	−3.07590	0.16960	2.41610
485	−0.02238	0.327225	1.34963	−3.07790	0.16938	2.41700
486	−0.02217	0.326875	1.33633	−3.07880	0.16916	2.39940
487	−0.02150	0.327163	1.34164	−3.07840	0.17053	2.42340
488	−0.02180	0.326804	1.33730	−3.07930	0.17032	2.42610
489	−0.02311	0.326587	1.33255	−3.08320	0.17042	2.42770
490	−0.02322	0.326659	1.32879	−3.08430	0.17120	2.43140
491	−0.02404	0.323020	1.34590	−3.08650	0.17104	2.43460
492	−0.02454	0.361030	1.22980	−3.08880	0.17119	2.44340
493	−0.02670	0.326050	1.31600	−3.09310	0.17182	2.44060
494	−0.02779	0.325650	1.31190	−3.09510	0.17160	2.44360
495	−0.02978	0.325360	1.30810	−3.09880	0.17160	2.44710
496	−0.03137	0.325260	1.30250	−3.10250	0.17210	2.44700
497	−0.03196	0.324830	1.29960	−3.10410	0.17190	2.45250
498	−0.03389	0.324470	1.29570	−3.10860	0.17180	2.45600
499	−0.03543	0.324338	1.29175	−3.11200	0.17231	2.45940
500	−0.03717	0.323894	1.28344	−3.11530	0.17220	2.45410

Table 2 (Continued)
Transfer matrix elements for beam line 2A

Energy (MeV)	Horizontal transfer matrix elements					
	R_{11} (cm/cm)	R_{12} (cm/mr)	R_{16} (cm/%)	R_{21} (mr/cm)	R_{22} (mr/mr)	R_{26} (mr/%)
501	−0.03685	0.323606	1.28355	−3.11450	0.17228	2.46520
502	−0.03801	0.323491	1.27943	−3.11700	0.17281	2.46820
503	−0.04033	0.323044	1.27514	−3.12170	0.17258	2.47050
504	−0.04437	0.322603	1.26301	−3.13040	0.17240	2.45630
505	−0.04374	0.322609	1.26652	−3.12880	0.17322	2.47630
506	−0.04607	0.322181	1.26233	−3.13280	0.17328	2.47980
507	−0.04879	0.322060	1.25807	−3.13730	0.17390	2.48250
508	−0.05819	0.321357	1.23957	−3.15670	0.17325	2.45540
509	−0.05526	0.321165	1.24952	−3.14980	0.17378	2.48880
510	−0.05904	0.320807	1.24010	−3.15670	0.17402	2.48220

Table 2 (Continued)
Transfer matrix elements for beam line 2A

Energy (MeV)	Vertical transfer matrix elements			
	R_{33} (cm/cm)	R_{34} (cm/mr)	R_{43} (mr/cm)	R_{44} (mr/mr)
470	1.13384	0.622629	0.47860	1.14480
471	1.13350	0.622692	0.47980	1.14582
472	1.13385	0.622872	0.48260	1.14707
473	1.13271	0.622784	0.48160	1.14763
474	1.13106	0.619960	0.48320	1.14898
475	1.12979	0.619842	0.48160	1.14937
476	1.12954	0.619895	0.48250	1.15011
477	1.12885	0.619861	0.48210	1.15057
478	1.12752	0.619721	0.48010	1.15077
479	1.12706	0.619724	0.48010	1.15124
480	1.12664	0.619845	0.48200	1.15277
481	1.12510	0.619659	0.47910	1.15268
482	1.12426	0.619583	0.47780	1.15281
483	1.12378	0.619568	0.47740	1.15305
484	1.12225	0.619381	0.47430	1.15284
485	1.12121	0.619273	0.47230	1.15276
486	1.11973	0.616431	0.47310	1.15351
487	1.11812	0.616255	0.46970	1.15322
488	1.11726	0.616142	0.46780	1.15301
489	1.11681	0.616097	0.46690	1.15295
490	1.11565	0.615927	0.46410	1.15254
491	1.11498	0.615824	0.46230	1.15223
492	1.11429	0.615832	0.46230	1.15292
493	1.11395	0.615779	0.46130	1.15268
494	1.11310	0.615636	0.45890	1.15218
495	1.11220	0.615489	0.45640	1.15163
496	1.11180	0.615398	0.45480	1.15118
497	1.11130	0.615300	0.45310	1.15066
498	1.11060	0.615151	0.45070	1.14998
499	1.10912	0.612189	0.44980	1.14989
500	1.10838	0.612023	0.44710	1.14908

Table 2 (Continued)
Transfer matrix elements for beam line 2A

Energy (MeV)	Vertical transfer matrix elements			
	R_{33} (cm/cm)	R_{34} (cm/mr)	R_{43} (mr/cm)	R_{44} (mr/mr)
501	1.10815	0.611940	0.44560	1.14846
502	1.10770	0.611812	0.44340	1.14767
503	1.10710	0.611658	0.44080	1.14682
504	1.10663	0.611519	0.43850	1.14595
505	1.10676	0.611576	0.43910	1.14617
506	1.10600	0.611372	0.43560	1.14495
507	1.10542	0.611209	0.43270	1.14386
508	1.10489	0.611009	0.42960	1.14266
509	1.10461	0.610834	0.42700	1.14144
510	1.10405	0.610608	0.42360	1.14005

Table 3

TRANSPORT listing for beam delivery of a 500 MeV beam to the west target (TGT2)

```
'97/12/29 - 500 MEV ON 2-A - TGT2 - FINAL COORDS + MEASURED Leff - NEW FF'
  0
 13.00      ' '          12.00000;
 16.00    '1/R1'         12.00000        0.00000;
 16.00    '1/R2'         13.00000        0.00000;
 16.00    'G/2 '          5.00000        5.08000;
 16.00    'X0 '          16.00000       -0.29135;
 16.00    'Z0 '          18.00000       11.07463;
 16.00    'T0 '          19.00000       35.10000;
  1.00    'BEAM'          0.12700        1.60000      0.66900      0.55600
                          0.00000        0.10000      1.09007;
 12.00     '12 '          0.00000        0.00000      0.00000      0.00000
                          0.00000       -0.96300      0.00000      0.00000
                          0.00000        0.00000      0.00000      0.00000
                          0.00000        0.00000      0.00000;
  1.00    'FOIL'          0.00000        0.17100      0.00000      0.17100
                          0.00000        0.00000      0.00000      0.00000
 14.00     'R1 '         -0.03717        0.32389      0.00000      0.00000
                          0.00000        1.28344      1.00000;
 14.00     'R2 '         -3.11530        0.17220      0.00000      0.00000
                          0.00000        2.45410      2.00000;
 14.00     'R3 '          0.00000        0.00000      1.10838      0.61202
                          0.00000        0.00000      3.00000;
 14.00     'R4 '          0.00000        0.00000      0.44710      1.14908
                          0.00000        0.00000      4.00000;
  3.00    'CMEX'         -0.59617;
  3.00      ' '           0.21004;
  3.00      ' '           0.31273;
  5.00    '2VQ1'          0.40234       -3.70003      5.08000;
  3.00      ' '           0.25654;
  5.00    '2VQ2'          0.40258        5.27964      5.08000;
  3.00      ' '           0.24181;
  3.00    'B1IN'          0.37190;
 20.00      ' '         180.00000;
  2.00      ' '          13.73589;
  4.00    'BEN1'          1.24595       13.99239      0.00000;
  2.00      ' '          13.73589;
 20.00      ' '        -180.00000;
  3.00    'B1EX'          0.00001;
  3.00      ' '           0.08972;
  3.00      ' '           0.27380;
  3.00      ' '           0.47174;
  3.00      ' '           0.27380;
```

Table 3 (continued)

3.00	'B2IN'	0.08727;			
20.00	' '	180.00000;			
2.00	' '	13.78220;			
4.00	'BEN2'	1.24595	14.03957	0.00000;	
2.00	' '	13.78220;			
20.00	' '	−180.00000;			
3.00	'B2EX'	0.00001;			
3.00	' '	1.00156;			
5.00	'2VQ3'	0.26288	5.74263	5.08000;	
3.00	' '	0.28952;			
5.00	'2VQ4'	0.26288	−4.69867	5.08000;	
3.00	' '	0.40900;			
3.00	' '	0.28796;			
3.00	' '	1.00000;			
3.00	' '	1.00000;			
3.00	'YWST'	1.00000;			
−10.00	'FYW1'	4.00000	3.00000	0.00000	0.00100;
−10.00	'SYW1'	3.00000	3.00000	0.66000	0.01000;
3.00	'XWST'	0.78321;			
−10.00	'FXW1'	2.00000	1.00000	0.00000	0.00100;
−10.00	'SXW1'	1.00000	1.00000	1.15000	0.01000;
3.00	' '	1.23290;			
3.00	' '	1.00181;			
5.00	'2VQ5'	0.26238	−1.66757	5.08000;	
3.00	' '	0.28989;			
5.00	'2VQ6'	0.26264	3.12881	5.08000;	
3.00	' '	0.28989;			
5.00	'2VQ7'	0.26238	−1.66757	5.08000;	
3.00	' '	1.00000;			
3.00	'WALL'	0.52437;			
−10.00	'ZFIT'	8.00000	1.00000	15.24000	0.00100;
3.00	'MID2'	0.92100;			
3.00	'WALX'	1.36500;			
3.00	' '	1.00000;			
3.00	' '	1.00000;			
3.00	' '	1.00000;			
3.00	' '	1.00000;			
3.00	' '	1.00000;			
3.00	' '	1.00000;			
3.00	' '	1.00000;			
3.00	'WST2'	1.00000;			
−10.00	'FXW2'	2.00000	1.00000	0.00000	0.00100;
−10.00	'FYW2'	4.00000	3.00000	0.00000	0.00100;
3.00	'TUNL'	1.12891;			
3.00	' '	1.00000;			

Table 3 (continued)

3.00	' '	0.87391;			
5.00	'2AQ8'	0.40336	−1.52876	5.08000;	
3.00	' '	0.31082;			
5.00	'2AQ9'	0.40260	2.65326	5.08000;	
3.00	' '	0.31082;			
5.00	'AQ10'	0.40336	−1.52876	5.08000;	
3.00	' '	0.96207;			
3.00	' '	0.96207;			
3.00	' '	1.04211;			
3.00	'WST3'	0.60000;			
−10.00	'FXW3'	2.00000	1.00000	0.00000	0.00100;
−10.00	'FYW3'	4.00000	3.00000	0.00000	0.00100;
−10.00	'SYW3'	3.00000	3.00000	0.29100	0.00500;
3.00	' '	1.00000;			
3.00	' '	1.00000;			
3.00	' '	1.13530;			
5.00	'AQ11'	0.26200	2.35098	5.08000;	
3.00	' '	0.29040;			
5.00	'AQ12'	0.26200	−2.65413	5.08000;	
3.00	' '	1.13530;			
3.00	' '	1.00000;			
3.00	'WST4'	1.00000;			
3.00	' '	1.08211;			
3.00	' '	1.08211;			
3.00	' '	1.08211;			
3.00	' '	1.07570;			
5.00	'AQ13'	0.26276	2.97431	5.08000;	
3.00	' '	0.28964;			
5.00	'AQ14'	0.26276	−3.32669	5.08000;	
3.00	' '	1.07570;			
3.00	' '	1.08211;			
3.00	' '	1.08211;			
3.00	' '	−0.13065;			
3.00	'B3IN'	1.08211;			
20.00	' '	180.00000;			
2.00	' '	7.50000;			
4.00	'BEN3'	0.94269	10.09781	0.00000;	
2.00	' '	7.50000;			
20.00	' '	−180.00000;			
3.00	'B3EX'	0.00001;			
3.00	' '	0.75000;			
3.00	' '	0.46516 ;			
3.00	'B4IN'	0.75000;			

Table 3 (continued)

20.00	' '	180.00000;			
2.00	' '	7.50000;			
4.00	'BEN4'	0.94269	10.09781	0.00000;	
2.00	' '	7.50000;			
20.00	' '	−180.00000;			
3.00	'B4EX'	0.00001;			
3.00	' '	0.25000;			
3.00	' '	0.25000;			
3.00	' '	0.25661;			
5.00	'AQ15'	0.26200	5.49717	5.08000;	
3.00	' '	0.29040;			
5.00	'AQ16'	0.26200	−5.74980	5.08000;	
3.00	' '	0.38903;			
3.00	' '	0.50000;			
3.00	' '	0.50000;			
3.00	' '	0.50000;			
3.00	' '	0.50000;			
−10.00	' '	4.00000	3.00000	0.00000	0.00100;
3.00	'TGT2'	0.50000;			
−10.00	' '	−1.00000	6.00000	0.06000	0.00100;
−10.00	' '	1.00000	1.00000	0.15000	0.01000;
−10.20	' '	3.00000	3.00000	0.2o000	0.01000;
−10.00	'ZFIT'	8.00000	1.00000	57.89894	0.00100;
−10.00	'ZFIT'	8.00000	3.00000	10.79279	0.00100;

Table 4

Element settings as a function of energy for beam line 2A

Element	Field (kG) at energy					
	480 MeV		489 MeV		490 MeV	
2AVQ1	−3.61958		−3.65556		−3.65836	
2AVQ2	5.12315		5.19158		5.19676	
2AVB1	13.65197		13.80563		13.82257	
2AVB2	13.69801		13.85217		13.86917	
2AVQ3	5.63000		5.68120		5.68775	
2AVQ4	−4.60934		−4.64886		−4.65369	
2AVQ5	−1.62014		−1.64255		−1.64357	
2AVQ6	3.03644		3.08018		3.08224	
2AVQ7	−1.62014		−1.64255		−1.64357	
2AQ8	−1.48957		−1.50790		−1.50874	
2VQ9	2.58345		2.61613		2.61757	
2Q10	−1.48957		−1.50790		−1.50874	
2AQ11	2.28490		2.31810		2.31810	
2AQ12	−2.58512		−2.62015		−2.62015	
2AQ13[a)]	2.97431	4.66087	2.97431	4.83671	2.97431	4.83671
2AQ14[a)]	−3.32807	−4.39969	−3.33011	−4.47800	−3.32888	−4.47627
2AB3	9.97525		9.96302		9.97525	
2AB4	9.97525		9.96302		9.97525	
2AQ15/17[a)]	5.40339	6.75236	5.45166	6.70711	5.45166	6.70711
2AQ16/18[a)]	−5.74980	−6.56508	−5.75849	−6.45524	−5.74980	−6.43893

[a)] Two field values are listed for quadrupoles 2AQ13 through 2AQ16. At a given energy, the left value refers to beam delivery to the target labelled TGT2 (the west target) and the right to beam delivery to that labelled TGT1 (the east target).

Table 4 (Continued)

Element settings as a function of energy for beam line 2A

Element	Field (kG) at energy					
	491 MeV		492 MeV		500 MeV	
2AVQ1	−3.66762		−3.61377		−3.70003	
2AVQ2	5.22046		5.05513		5.27964	
2AVB1	13.83964		13.85671		13.99239	
2AVB2	13.88630		13.90343		14.03957	
2AVQ3	5.68634		5.77874		5.74263	
2AVQ4	−4.65396		−4.70781		−4.69867	
2AVQ5	−1.64609		−1.64943		−1.66757	
2AVQ6	3.08625		3.09318		3.12881	
2AVQ7	−1.64609		−1.64943		−1.66757	
2AQ8	−1.51317		−1.51570		−1.52876	
2VQ9	2.62451		2.62913		2.65326	
2Q10	−1.51317		−1.51570		−1.52876	
2AQ11	2.32226		2.33274		2.35098	
2AQ12	−2.62534		−2.63673		−2.65413	
2AQ13[a)]	2.97431	4.83671	2.97431	4.83671	2.97431	4.74900
2AQ14[a)]	−3.32902	−4.47567	−3.32185	−4.47507	−3.32669	−4.45293
2AB3	9.98758		9.99990		10.09781	
2AB4	9.98758		9.99990		10.09781	
2AQ15/17[a)]	5.45204	6.71051	5.50378	6.72470	5.49717	6.86696
2AQ16/18[a)]	−5.75212	−6.43428	−5.74685	−6.42983	−5.74980	−6.59686

[a)] Two field values are listed for quadrupoles 2AQ13 through 2AQ16. At a given energy, the left value refers to beam delivery to the target labelled TGT2 (the west target) and the right to beam delivery to that labelled TGT1 (the east target).

Table 5

Beam sizes at the waist locations

Waist	Parameter	480 MeV	489 MeV	490 MeV	491 MeV	492 MeV	500 MeV
WST1	$\pm x$ (cm)	1.150	1.150	1.150	1.150	1.150	1.150
	$\pm\theta$ (mr)	0.352	0.355	0.355	0.355	0.357	0.359
	$\pm y$ (cm)	0.660	0.660	0.660	0.660	0.660	0.660
	$\pm\phi$ (mr)	0.230	0.230	0.230	0.230	0.230	0.230
WST2	$\pm x$ (cm)	1.051	1.047	1.048	1.048	1.047	1.045
	$\pm\theta$ (mr)	0.385	0.390	0.390	0.330	0.392	0.396
	$\pm y$ (cm)	0.331	0.331	0.331	0.331	0.331	0.331
	$\pm\phi$ (mr)	0.459	0.459	0.459	0.460	0.460	0.459
WST3	$\pm x$ (cm)	1.047	1.043	1.045	1.045	1.044	1.041
	$\pm\theta$ (mr)	0.386	0.392	0.391	0.391	0.393	0.397
	$\pm y$ (cm)	0.293	0.293	0.293	0.293	0.293	0.293
	$\pm\phi$ (mr)	0.519	0.519	0.519	0.519	0.520	0.519
WST4	$\pm x$ (cm)	0.853	0.848	0.850	0.851	0.849	0.847
	$\pm\theta$ (mr)	0.474	0.482	0.480	0.480	0.483	0.488
	$\pm y$ (cm)	0.397	0.397	0.397	0.397	0.396	0.397
	$\pm\phi$ (mr)	0.383	0.383	0.383	0.383	0.384	0.383

Table 6

Beam sizes and overall transfer matrices at the TGT2 (west target) location

Parameter	480 MeV	489 MeV	490 MeV	491 MeV	492 MeV	500 MeV
$\pm x$ (cm)	0.160	0.155	0.156	0.155	0.164	0.151
$\pm\theta$ (mr)	1.412	1.446	1.449	1.445	1.518	1.490
$\pm y$ (cm)	0.200	0.200	0.201	0.203	0.201	0.201
$\pm\phi$ (mr)	0.761	0.759	0.758	0.765	0.758	0.758
R_{11} (cm/cm)	−0.8814	−0.8513	−0.8508	−0.8355	−1.0035	−0.8463
R_{12} (cm/mr)	0.0709	0.0693	0.0695	0.0698	0.0642	0.0656
R_{16} (cm/%)	0.0002	0.0000	−0.0001	0.0000	0.0000	0.0000
R_{21} (mr/cm)	−7.0730	−7.0189	−7.0492	−6.9874	−7.7980	−6.9897
R_{22} (mr/mr)	−0.5723	−0.6066	−0.6034	−0.6045	−0.6079	−0.6426
R_{26} (mr/%)	5.8244	5.8688	5.9603	5.9570	6.0669	6.0110
R_{33} (cm/cm)	−0.3154	−0.2869	−0.2810	−0.2816	−0.2694	−0.2489
R_{34} (mr/cm)	−0.0206	0.0158	0.0237	0.0224	0.0383	0.0635
R_{43} (mr/cm)	−2.6814	−2.7259	−2.7354	−2.7401	−2.7486	−2.7865
R_{44} (cm/cm)	−3.3459	−3.3355	−3.3278	−3.3329	−3.3219	−3.3070

Table 7

Beam sizes and overall transfer matrices at the TGT1 (east target) location

Parameter	480 MeV	489 MeV	490 MeV	491 MeV	492 MeV	500 MeV
$\pm x$ (cm)	0.182	0.160	0.160	0.159	0.171	0.181
$\pm \theta$ (mr)	2.982	3.254	3.258	3.251	3.278	2.975
$\pm y$ (cm)	0.202	0.203	0.203	0.203	0.203	0.200
$\pm \phi$ (mr)	0.754	0.754	0.753	0.754	0.753	0.763
R_{11} (cm/cm)	0.2495	0.3163	0.3149	0.3061	0.3766	0.2463
R_{12} (cm/mr)	−0.1115	−0.0963	−0.0965	−0.0961	−0.1023	−0.1106
R_{16} (cm/%)	−0.0003	0.0000	0.0001	0.0000	0.0001	0.0003
R_{21} (mr/cm)	10.3783	12.0063	12.0033	11.8633	13.0264	10.3101
R_{22} (mr/mr)	−0.6069	−0.4852	−0.4915	−0.4819	−0.5891	−0.5598
R_{26} (mr/%)	−24.8997	−27.6605	−27.6893	−27.7430	−26.6612	−25.1445
R_{33} (cm/cm)	−0.3879	−0.3370	−0.3286	−0.3261	−0.3249	−0.3286
R_{34} (mr/cm)	−0.1106	−0.0428	−0.0313	−0.0282	−0.0265	−0.0373
R_{43} (mr/cm)	−2.5049	−2.7150	−2.7303	−2.7394	−2.7375	−2.7357
R_{44} (cm/cm)	−3.2924	−3.3125	−3.3027	−3.3038	−3.3016	−3.3532

Table 8

Estimated current settings for the beam line 2A transport elements as a function of energy

TRANSPORT settings for 500 MeV				TRANSPORT settings for 492 MeV			
Element	Field (kG)	Current (A) Fit to 2AVQ1	Current (A) Fit to 2AVQ2	Element	Field (kG)	Current (A) Fit to 2AVQ1	Current (A) Fit to 2AVQ2
2ACM1	−1.2446	−64.196		2ACM1	−0.0488	−9.031	
2AVQ1	−3.7000	209.251		2AVQ1	−3.6138	204.283	
2AVQ2	5.2796		298.007	2AVQ2	5.0551		284.956
2AVB1	13.9924	553.201		2AVB1	13.8567	546.431	
2AVB2	14.0396	555.576		2AVB2	13.9034	548.751	
2AVQ3	5.7426	202.422		2AVQ3	5.7787	203.814	
2AVQ4	−4.6987	163.818		2AVQ4	−4.7078	164.147	
2AVQ5	−1.6676	57.303		2AVQ5	−1.6494	56.672	
2AVQ6	3.1288	107.863		2AVQ6	3.0932	106.614	
2AVQ7	−1.6676	57.303		2AVQ7	−1.6494	57.672	
2AQ8	−1.5288	86.230	85.134	2AQ8	−1.5157	85.501	84.410
2AQ9	2.6533	149.398	147.799	2AQ9	2.6291	148.026	146.440
2AQ10	−1.5288	86.230	85.134	2AQ10	−1.5157	85.501	84.410
2AQ11	2.3510	80.837		2AQ11	2.3327	80.207	
2AQ12	−2.6541	91.308		2AQ12	−2.6367	90.705	
2AQ13	2.9743	102.452		2AQ13	2.9743	102.452	
2AQ14	−3.3267	114.825		2AQ14	−3.3219	114.656	
2AB3	10.0978	524.342		2AB3	9.9999	518.898	
2AB4	10.0978	524.342		2AB4	9.9999	518.898	
2AQ15	5.4972	193.105		2AQ15	5.5038	193.353	
2AQ16	−5.7498	202.699		2AQ16	−5.7469	202.588	

Table 8 (Continued)

Estimated current settings for the beam line 2A transport elements as a function of energy

TRANSPORT settings for 491 MeV				TRANSPORT settings for 490 MeV			
Element	Field (kG)	Current (A) Fit to 2AVQ1	Fit to 2AVQ2	Element	Field (kG)	Current (A) Fit to 2AVQ1	Fit to 2AVQ2
2ACM1	0.0983	11.118		2ACM1	0.2478	17.544	
2AVQ1	−3.6676	207.383		2AVQ1	−3.6584	206.853	
2AVQ2	5.2205		294.568	2AVQ2	5.1968		293.189
2AVB1	13.8396	545.583		2AVB1	13.8226	544.743	
2AVB2	13.8863	547.900		2AVB2	13.8692	547.051	
2AVQ3	5.6863	200.264		2AVQ3	5.6877	200.318	
2AVQ4	−4.6540	162.204		2AVQ4	−4.6537	162.193	
2AQ5	−1.6461	56.557		2AQ5	−1.6436	56.471	
2AQ6	3.0863	106.372		2AQ6	3.0822	106.229	
2AQ7	−1.6461	56.557		2AQ7	−1.6436	56.471	
2AQ8	−1.5132	85.362	84.272	2AQ8	−1.5087	85.112	84.023
2AQ9	2.6245	147.766	146.182	2AQ9	2.6176	147.375	145.795
2AQ10	−1.5132	85.362	84.272	2AQ10	−1.5087	85.112	84.023
2AQ11	2.3223	79.849		2AQ11	2.3181	79.704	
2AQ12	−2.6253	90.311		2AQ12	−2.6202	90.134	
2AQ13	2.9743	102.452		2AQ13	2.9743	102.452	
2AQ14	−3.3290	114.906		2AQ14	−3.3289	114.902	
2AB3	9.9876	518.215		2AB3	9.9753	517.533	
2AB4	9.9876	518.215		2AB4	9.9753	517.533	
2AQ15	5.4520	191.412		2AQ15	5.4517	191.401	
2AQ16	−5.7521	202.788		2AQ16	−5.7498	202.699	

Table 8 (Continued)

Estimated current settings for the beam line 2A transport elements as a function of energy

TRANSPORT settings for 489 MeV				TRANSPORT settings for 480 MeV			
Element	Field (kG)	Current (A) Fit to 2AVQ1	Fit to 2AVQ2	Element	Field (kG)	Current (A) Fit to 2AVQ1	Fit to 2AVQ2
2ACM1	0.3952	24.045		2ACM1	1.7258	88.440	
2AVQ1	−3.6556	206.691		2AVQ1	−3.6196	204.617	
2AVQ2	5.1916		292.887	2AVQ2	5.1231		288.905
2AVB1	13.8056	543.903		2AVB1	13.6520	536.377	
2AVB2	13.8522	546.208		2AVB2	13.6980	538.620	
2AVQ3	5.6812	200.069		2AVQ3	5.6300	198.119	
2AVQ4	−4.6489	162.020		2AVQ4	−4.6093	160.592	
2AQ5	−1.6425	56.432		2AQ5	−1.6201	55.655	
2AQ6	3.0802	106.159		2AQ6	3.0364	104.624	
2AQ7	−1.6425	56.432		2AQ7	−1.6201	55.655	
2AQ8	−1.5079	85.067	83.979	2AQ8	−1.4896	84.049	82.967
2AQ9	2.6161	147.290	145.711	2AQ9	2.5835	145.443	143.881
2AQ10	−1.5079	85.067	83.979	2AQ10	−1.4896	84.049	82.967
2AQ11	2.3181	79.704		2AQ11	2.2849	78.562	
2AQ12	−2.6202	90.134		2AQ12	−2.5851	88.919	
2AQ13	2.9743	102.452		2AQ13	2.9743	102.452	
2AQ14	−3.3301	114.945		2AQ14	−3.3281	114.874	
2AB3	9.9630	516.852		2AB3	9.9753	517.533	
2AB4	9.9630	516.852		2AB4	9.9753	517.533	
2AQ15	5.4517	191.401		2AQ15	5.4034	189.598	
2AQ16	−5.7585	203.035		2AQ16	−5.7498	202.699	

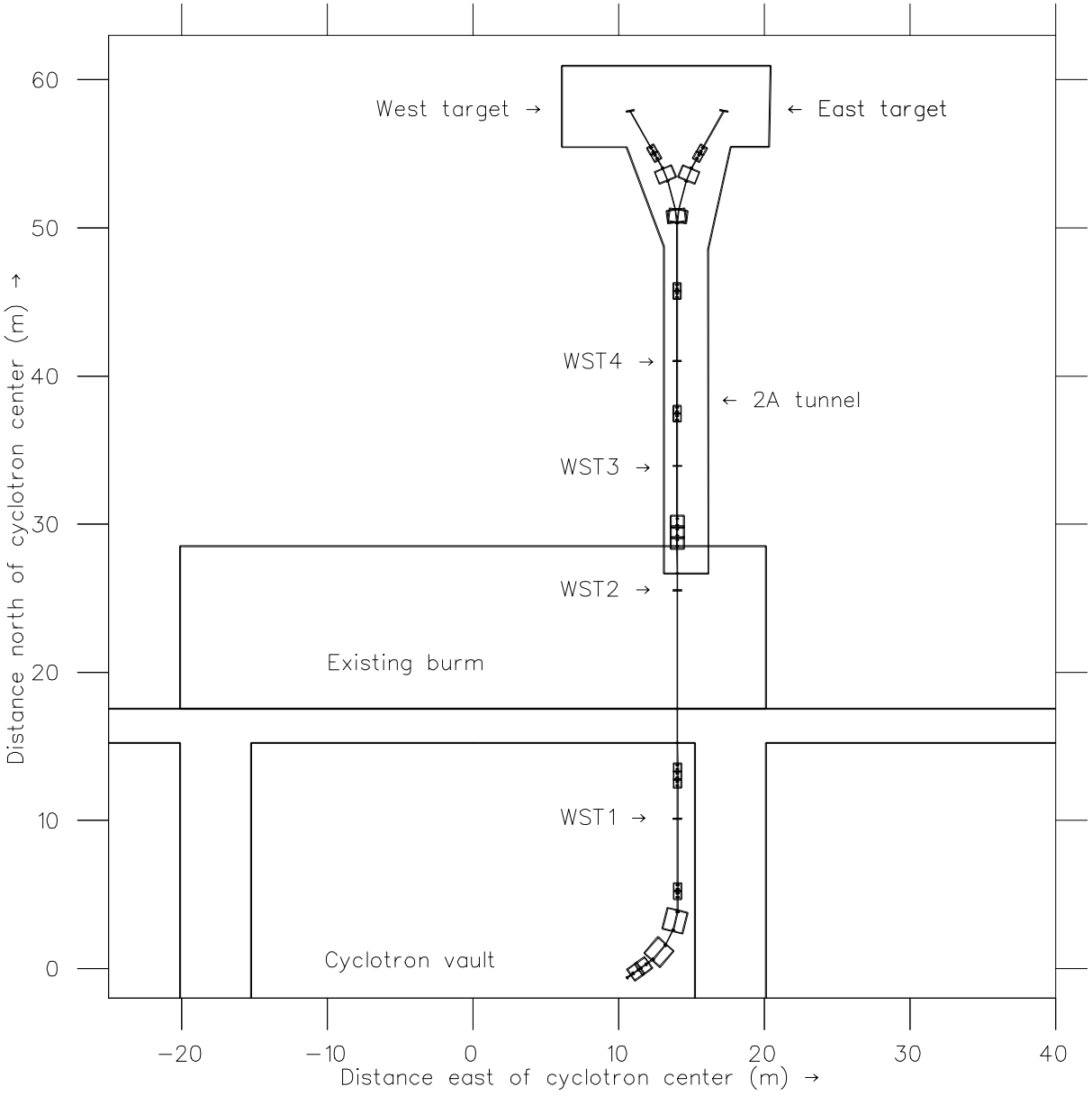

Fig. 1. The final configuration of beam line 2A.

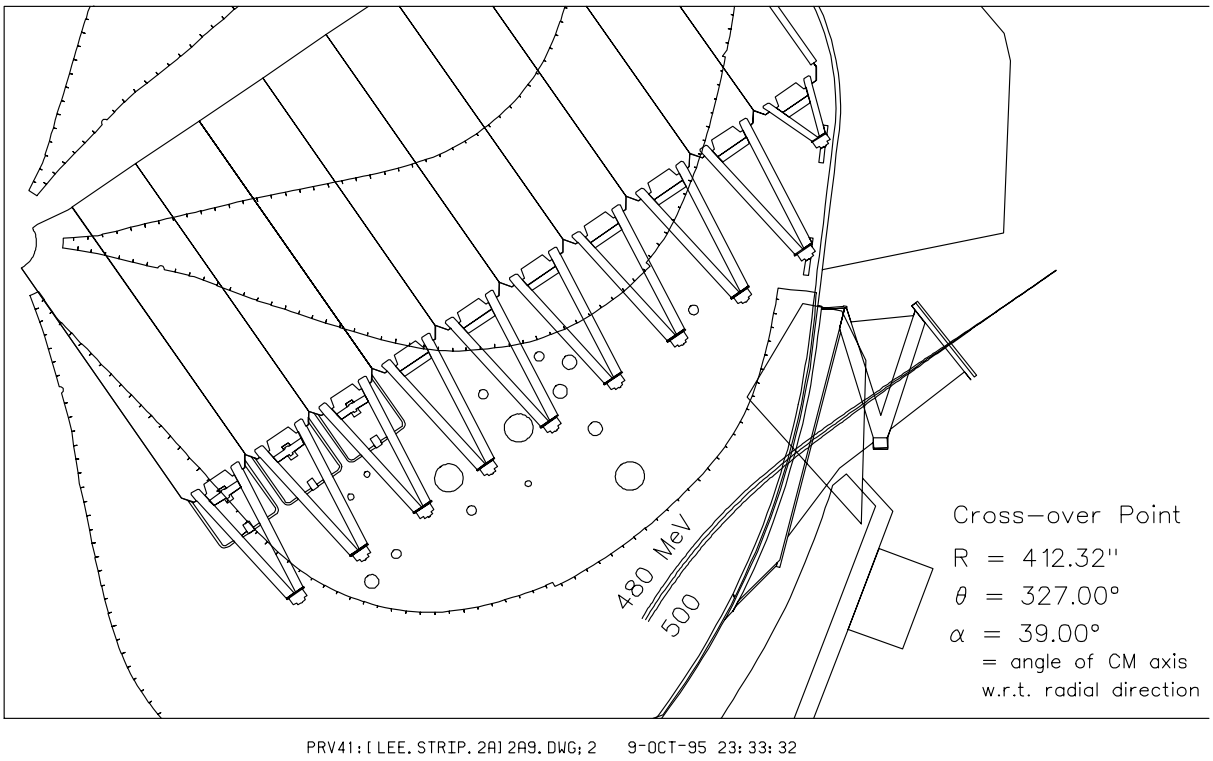

Fig. 2(a). The extraction trajectories for energies of 480, 490 and 500 MeV.

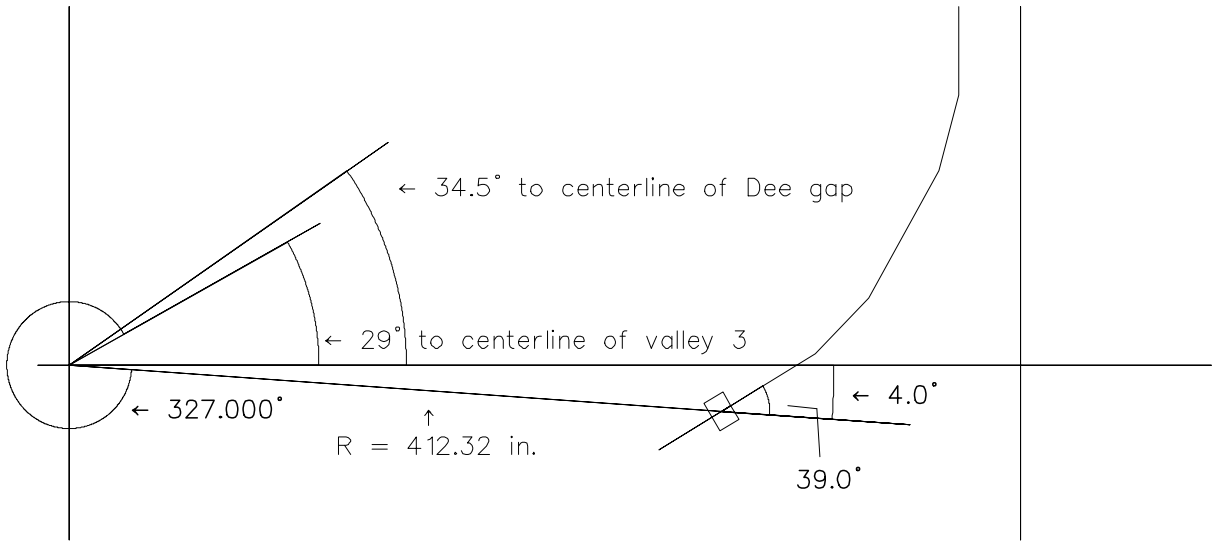

Fig. 2(b). The essential geometry of beam line 2A extraction.

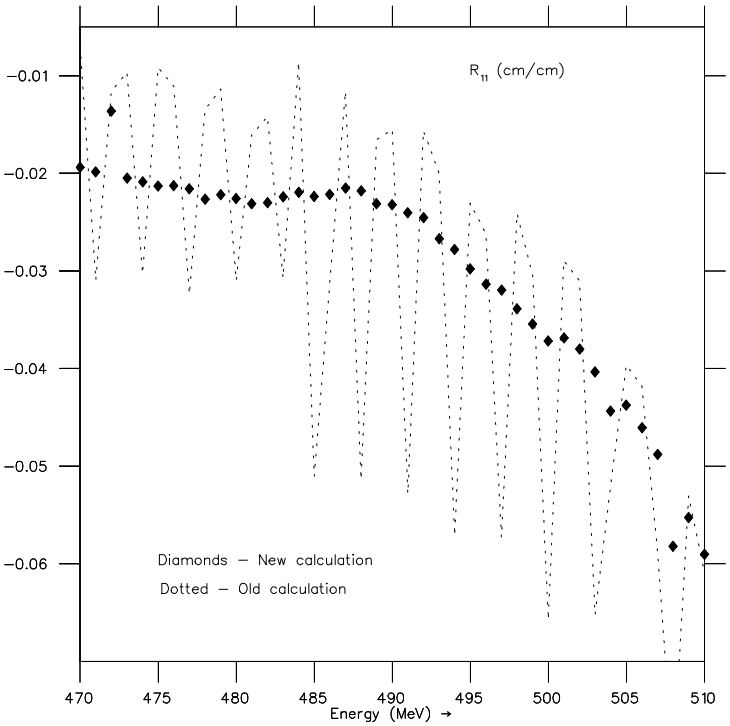

Fig. 3. Calculated values of R_{11} in units of cm/cm as a function of energy.

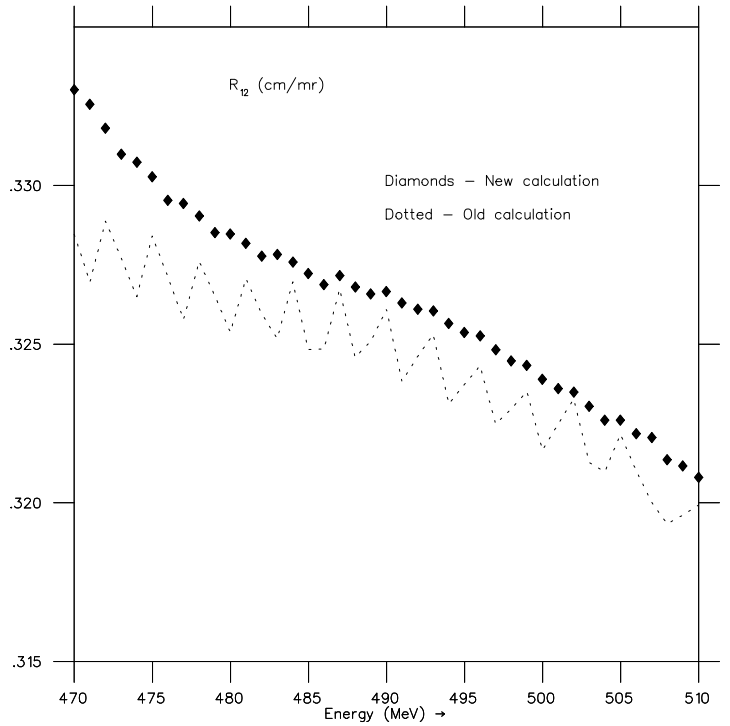

Fig. 4. Calculated values of R_{12} in units of cm/mr as a function of energy.

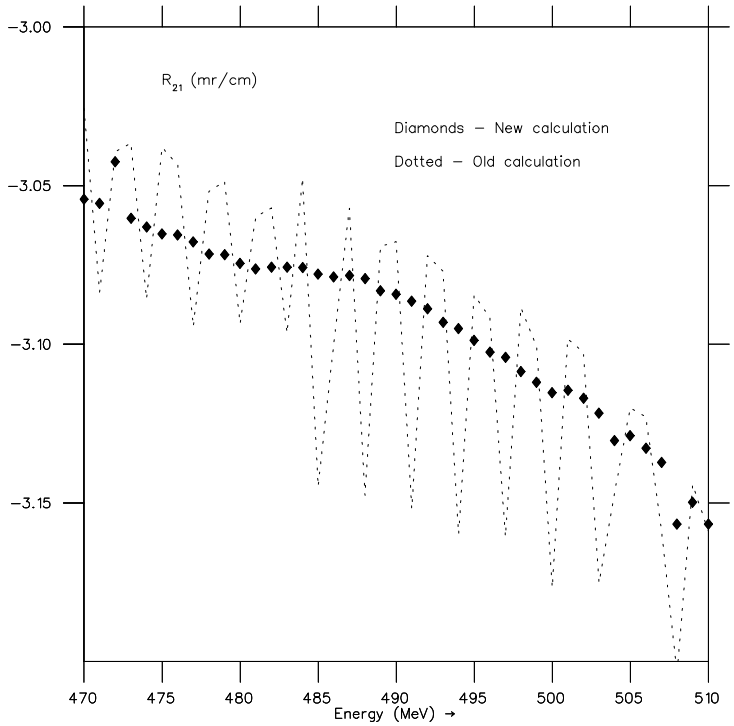

Fig. 5. Calculated values of R_{21} in units of mr/cm as a function of energy.

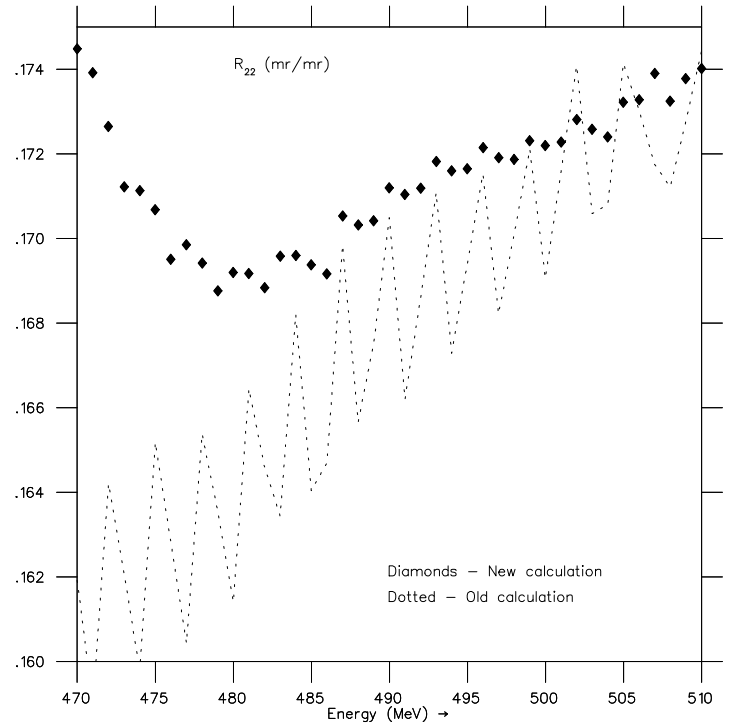

Fig. 6. Calculated values of R_{22} in units of mr/mr as a function of energy.

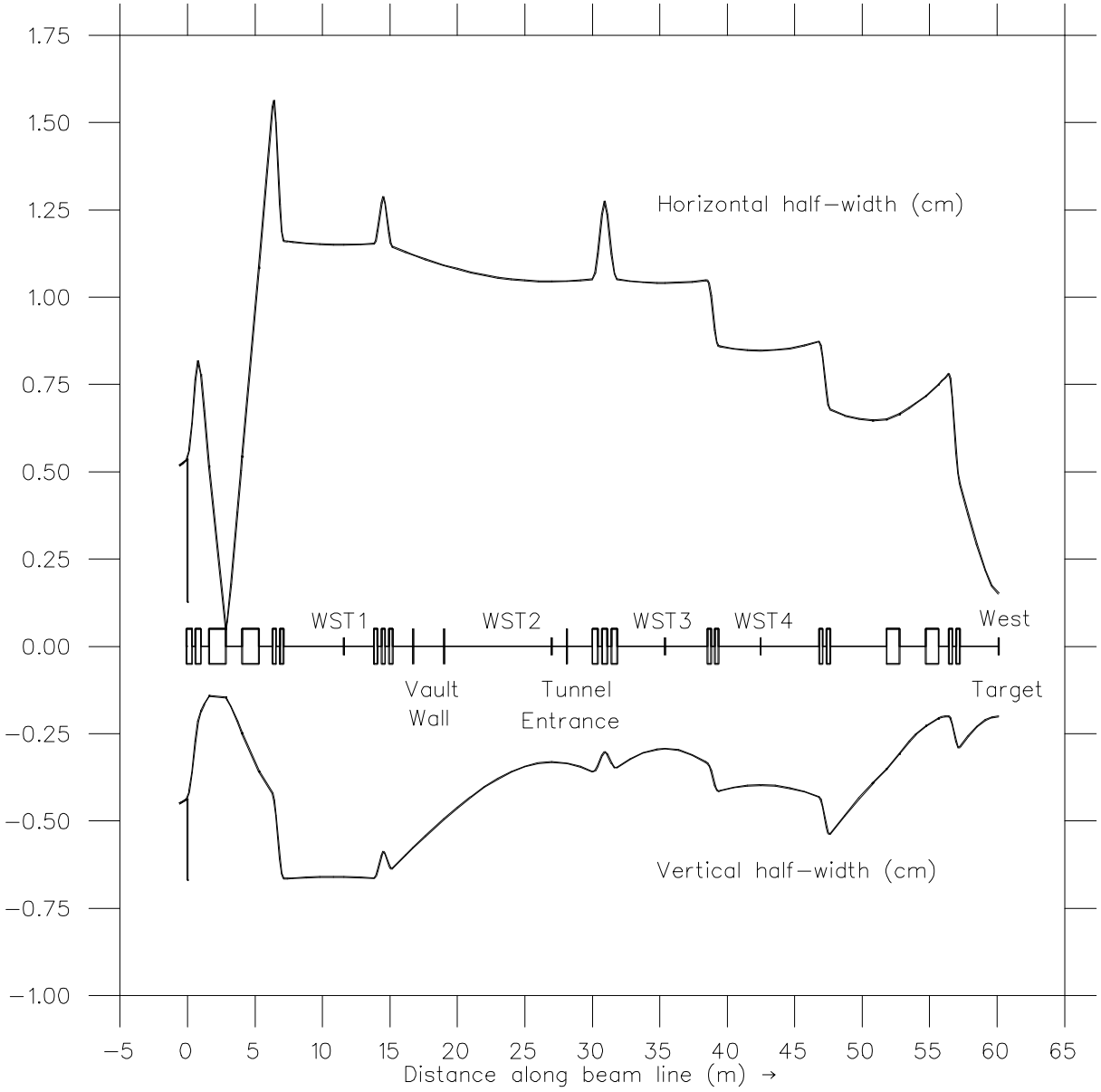

Fig. 7. Beam envelopes for beam delivery to the west target (TGT2) of beam line 2A.

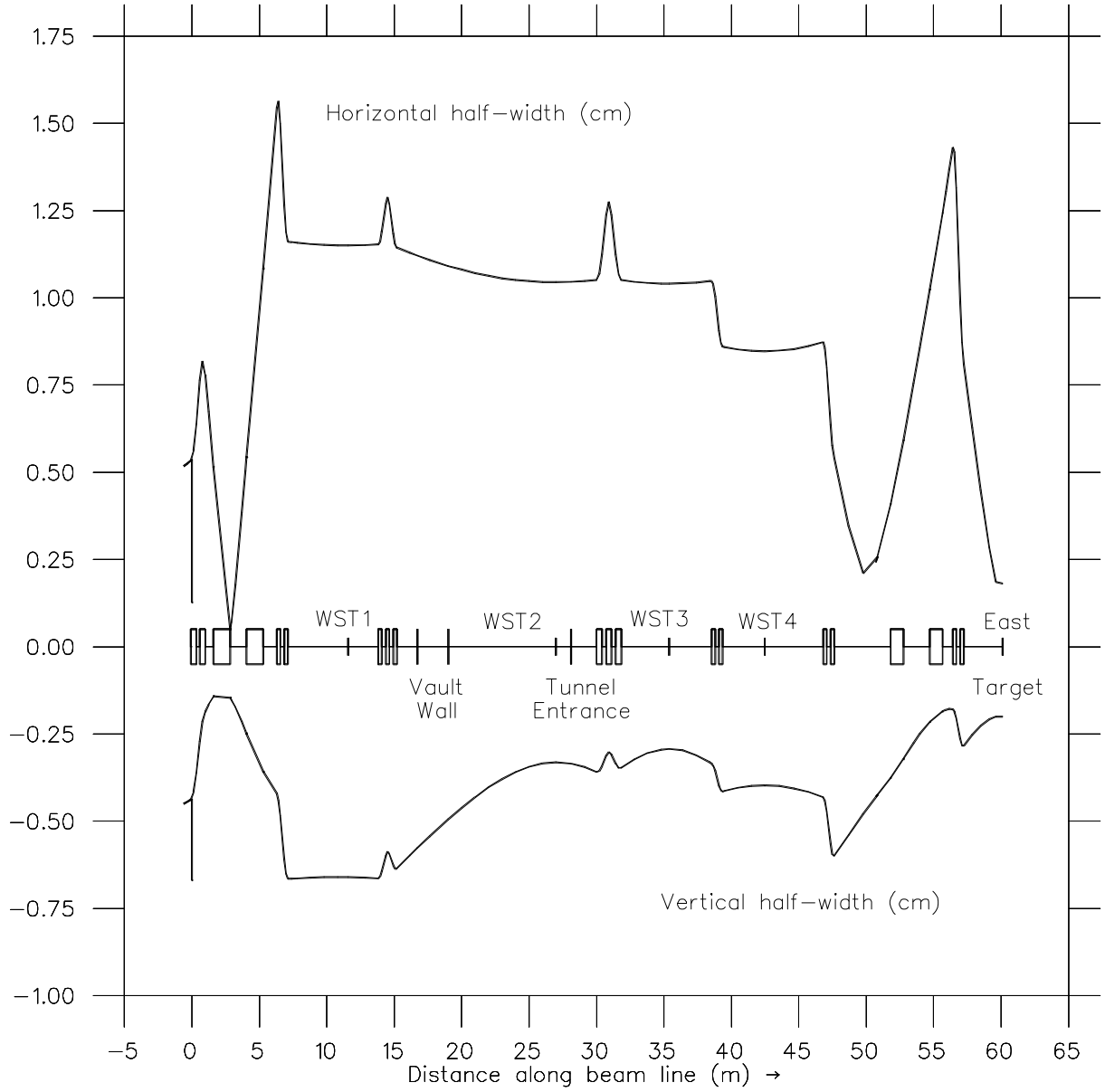

Fig. 8. Beam envelopes for beam delivery to the east target (TGT1) of beam line 2A.

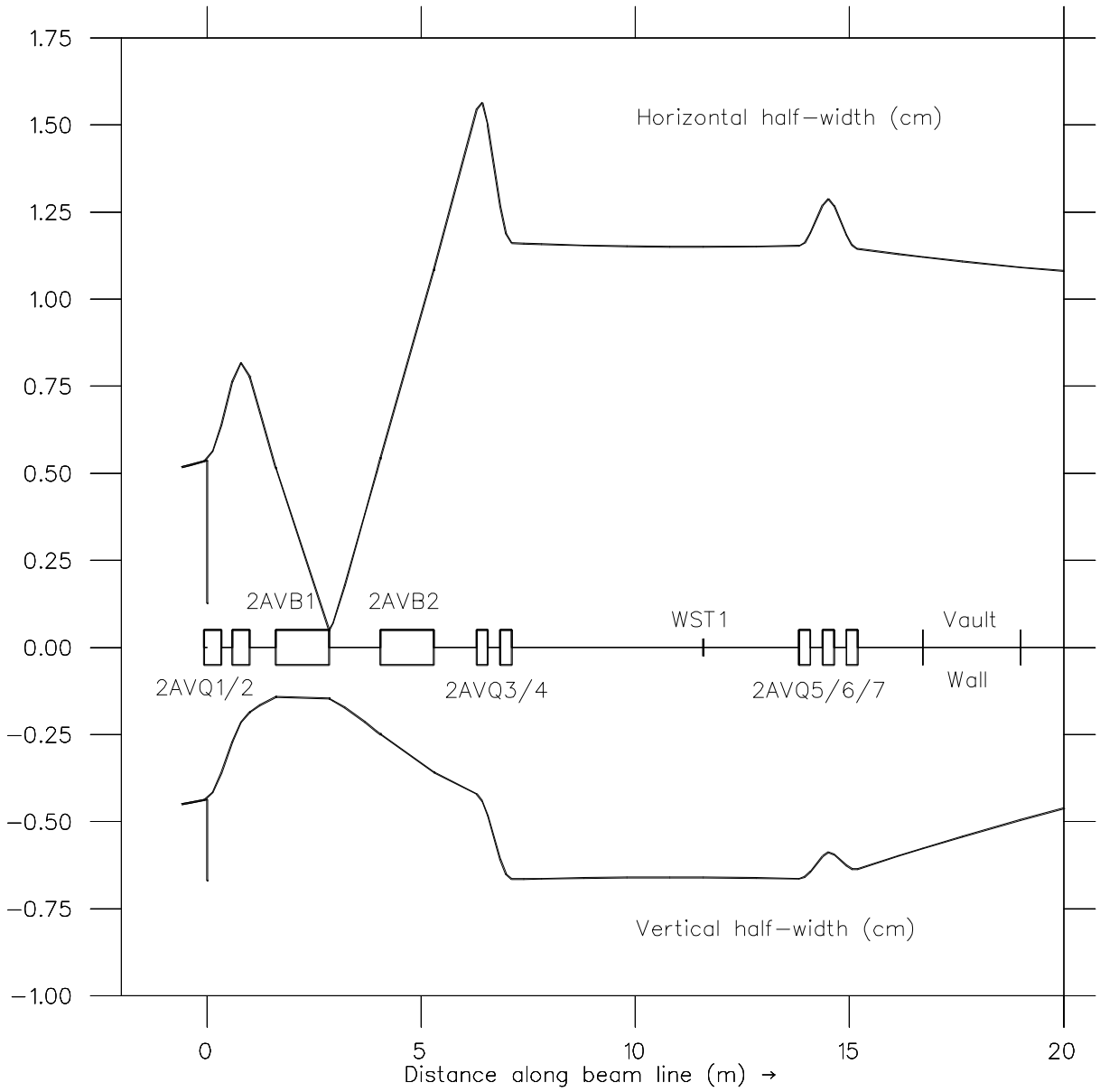

Fig. 9. Beam envelopes in the vault section of beam line 2A.

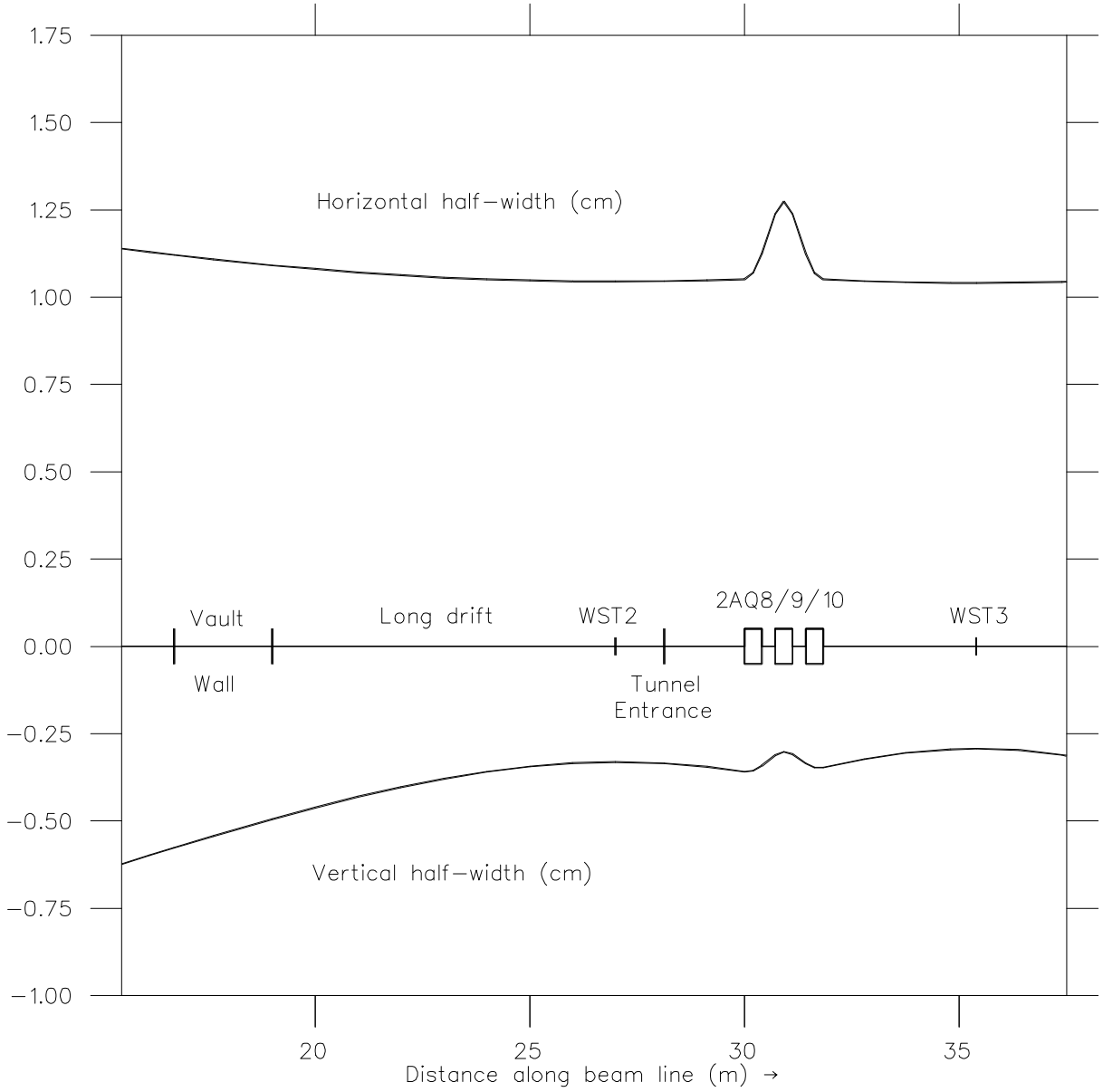

Fig. 10. Beam envelopes from the vault to the tunnel section of beam line

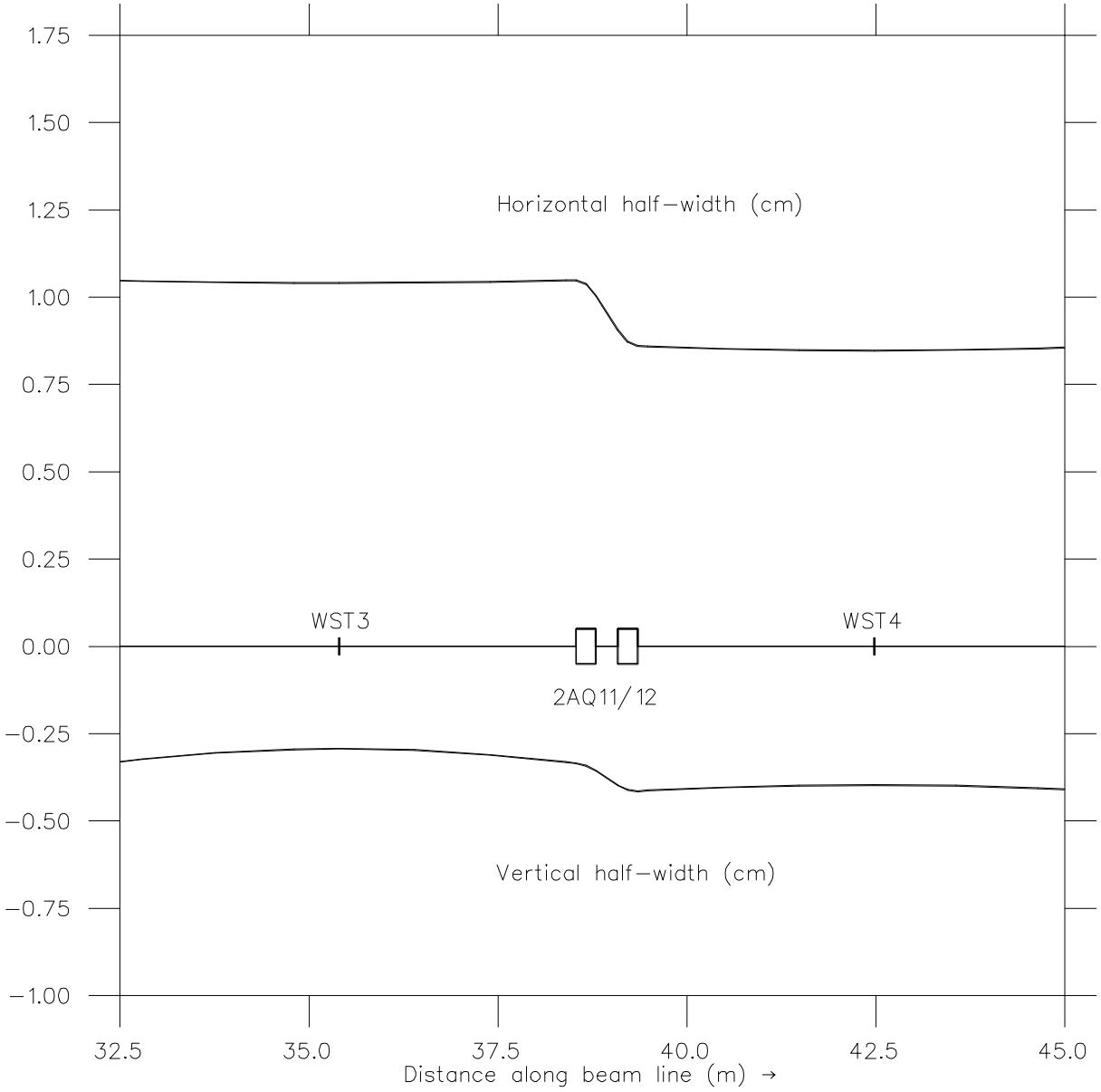

Fig. 11. Beam envelopes from the WST3 location to the WST4 location of beam line 2A.

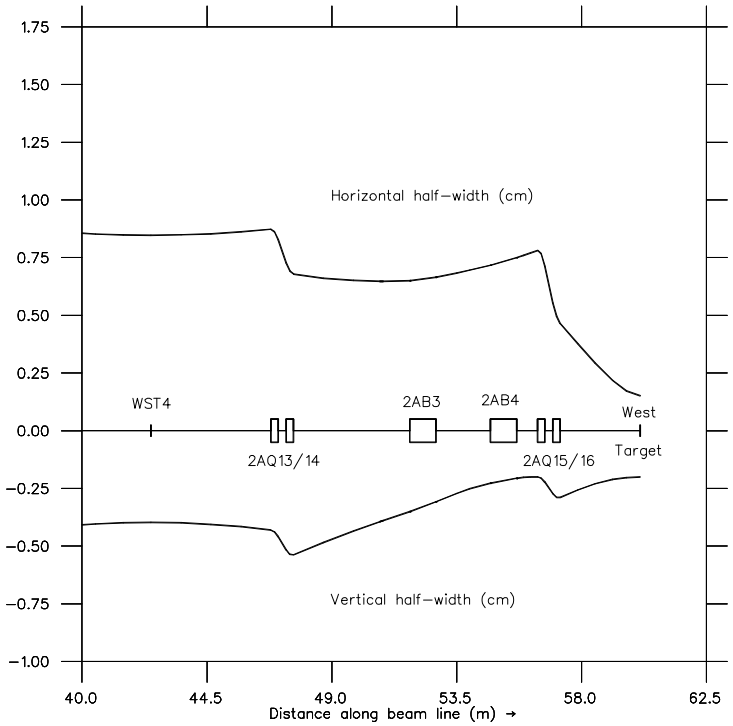

Fig. 12. Beam envelopes from the WST4 location to the west target (TGT2) location of beam line 2A.

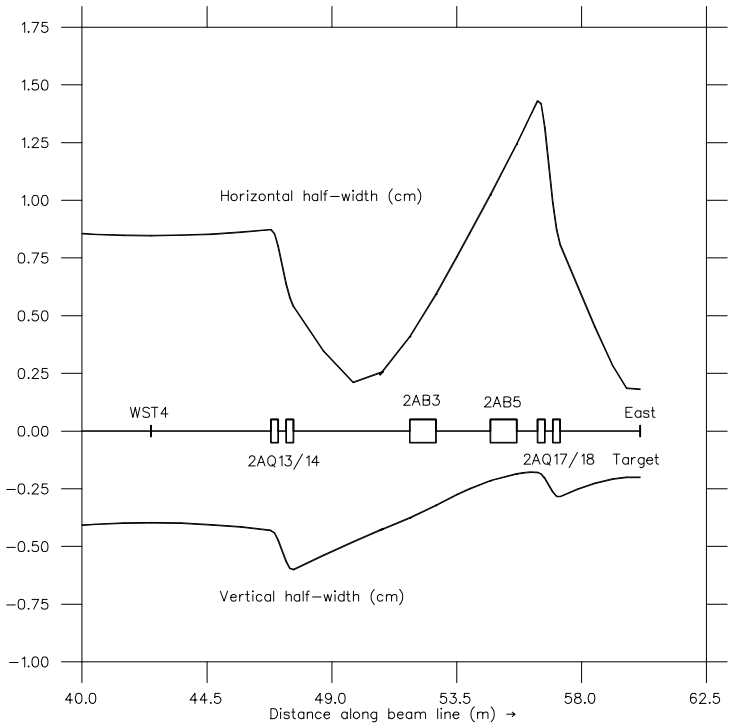

Fig. 13. Beam envelopes from the WST4 location to the east target (TGT1) location of beam line 2A.

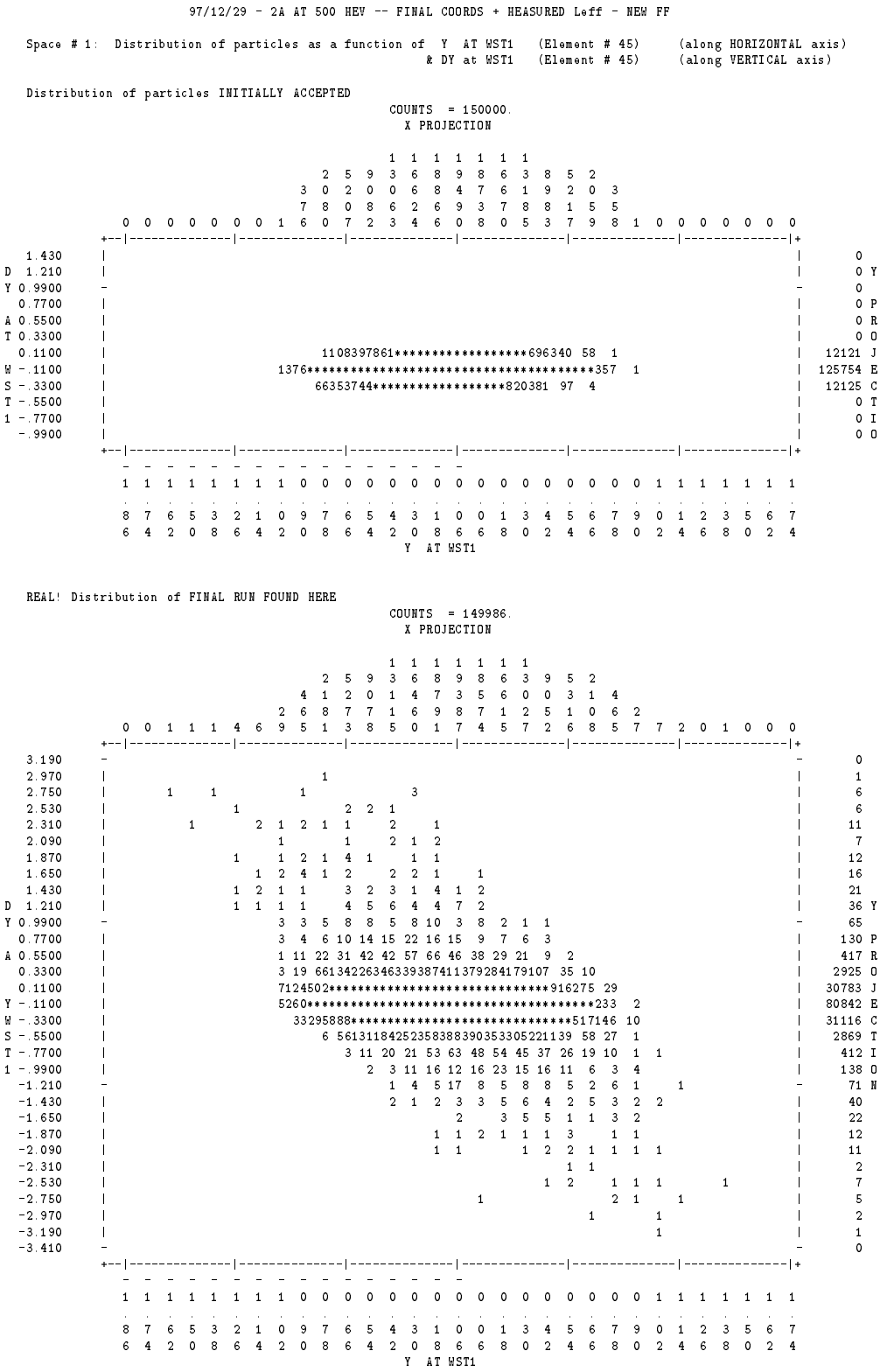

Fig. 14. The effect of scattering by the stripper foil on the vertical beam size at WST1. Upper: no scattering, Lower: with foil scattering.

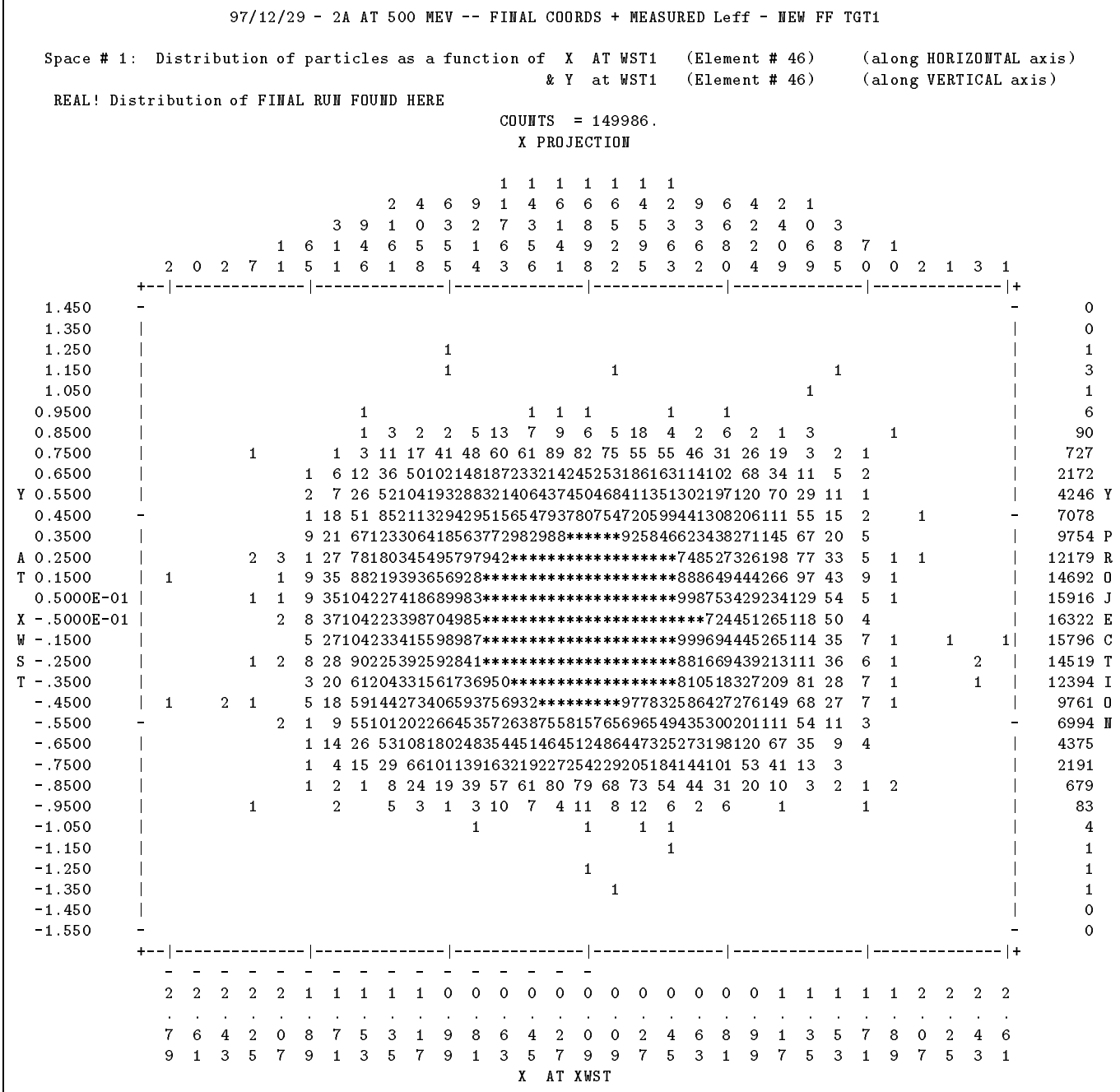

Fig. 15. The predicted beam spot at the WST1 location in the cyclotron vault.

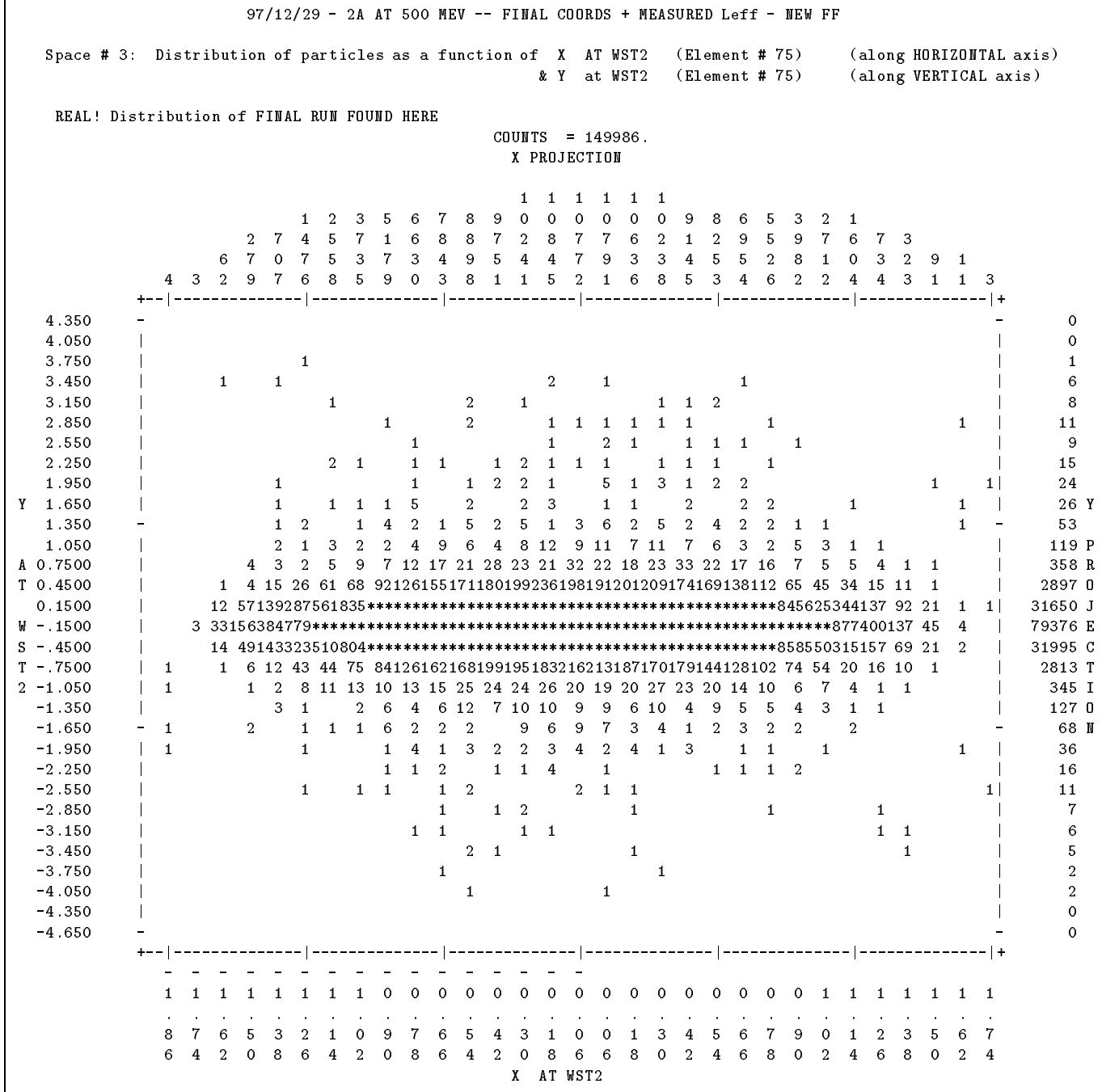

Fig. 16. The predicted beam spot at the WST2 location in the beam line 2A tunnel.

```
                    97/12/29 - 2A AT 500 MEV -- FINAL COORDS + MEASURED Leff - NEW FF

  Space # 4:  Distribution of particles as a function of  X  AT WST3   (Element # 93)     (along HORIZONTAL axis)
                                                          & Y  at WST3   (Element # 93)     (along VERTICAL axis)

   REAL! Distribution of FINAL RUN FOUND HERE
                                                  COUNTS  = 149986.
                                                    X PROJECTION

                                                                                  1     1
                                                 1  2  4  5  7  8  9  9  9  9  0  9  0  9  9  8  7  6  4  2  1
                                          1  6  3  5  0  6  0  3  3  5  8  9  0  9  0  8  5  6  5  1  4  8  5  6  1
                                       1  5  1  8  8  3  9  7  1  9  8  3  4  9  1  1  7  4  1  1  3  2  1  3  6  7  1
                                    0  0  6  3  8  4  9  1  7  3  2  4  1  9  4  9  4  8  3  9  6  2  4  9  3  9  5  9  5  0  0
                                   +--|-------------|-------------|-------------|-------------|-------------|-------------|+
     2.320                         -              1     1  1  1  1  1  1     1     1  4  2        1  1  1           1            -      19
     2.160                         |                          1              2        1     1                                  |       5
     2.000                         |                                      1                    2                            |       3
     1.840                         |                       1  1  1           2     2     2  1  2  2  2                       |      16
     1.680                         |                    1                       1        1        4        1           1  1    |      10
     1.520                         |                                   1  3     1  1     1  1  2  1     1  2  1        1       |      16
     1.360                         |                                   1        1  4     1  2  1  2  1  1                       |      14
     1.200                         |                    1     1  2  1  2  2  1  4  4  1     1  1  4  2           1  1          |      29
     1.040                         |                       2  1  2  4  1  6  3  4     2  1  4  3  2  1  3  1                    |      40
Y 0.8800                           |                 1        1  2  2  3  3  4  5  4  5  5  5  5  3  1  5  3  2              |      59 Y
  0.7200                           -                 1  1  4  3  6 12  5  6 12 10  9  8 13  9 12 10 11  8  7  3  6  4           -     160
  0.5600                           |                 2  4  3  8 23 22 21 25 19 31 17 29 19 19 24 26 25 16 19 11  4  1  2        |     370 P
A 0.4000                           |           1  1  7 15 30 46 60 91105107121119105112121117111122101 95 69 47 39 22 11  2        |    1777 R
T 0.2400                           |           1 11 42 99189279407513644695716691701740702773710713601547474305227112 66 12        |   10970 O
  0.8000E-01                       |           5 38144346612**********************************************************655357156 37  2     |   35641 J
W -.8000E-01                       |           2 48200477934**********************************************************963538226 70  7     |   51768 E
S -.2400                           |           6 39154323595948**********************************************************656365150 44  5     |   35473 C
T -.4000                           |           1 11 55 96170284426557587699745711698740750711757690654571439311210106 40  7  1     |   11027 T
3 -.5600                           |              4  9 14 29 39 66102101112128137112119119153115127102 86 77 50 35 28  9  5        |    1878 I
  -.7200                           |                 1  4 11 10  6 16 20 21 15 25 34 31 23 22 20 23 18 22 15 10  7  3              |     357 O
  -.8800                           -              1     1  5  5  7  3 10  9  8  6  7  5  9  7  9 10 13  6  9  5  3  1           -     139 N
  -1.040                           |                 1     2  4  1  7  6  4  7 10  9  2  6  4  4  3  1  3  1  2     1           |      78
  -1.200                           |                 1  1  1  2  2  1  3  2  2  2  4  4  2  1  1  3  3                 1           |      36
  -1.360                           |                 1     2  1  1     3     6  1  2  3  1  1     1  2  3  3     2     1           |      34
  -1.520                           |                       1     1  1  5  1  1  1  1  2  2  1  1  1  1              |      20
  -1.680                           |                          1     2  2     1  1     2  3              2                       |      14
  -1.840                           |                          1     1  1        1  1        1  2                                 |       8
  -2.000                           |                          2           1                          1              1         |       5
  -2.160                           |                                   2     2                    1                          |       5
  -2.320                           |                          1                                 1              2               |       4
  -2.480                           -                          2  2        1  1           2  2                 1               -      11
                                   +--|-------------|-------------|-------------|-------------|-------------|-------------|+
                                      -  -  -  -  -  -  -  -  -  -  -  -  -  -  -  -  -
                                      1  1  1  1  1  1  1  1  0  0  0  0  0  0  0  0  0  0  0  0  0  0  0  0  0  1  1  1  1  1  1  1
                                      .  .  .  .  .  .  .  .  .  .  .  .  .  .  .  .  .  .  .  .  .  .  .  .  .  .  .  .  .  .  .  .
                                      8  7  6  5  3  2  1  0  9  7  6  5  4  3  1  0  0  1  3  4  5  6  7  9  0  1  2  3  5  6  7
                                      6  4  2  0  8  6  4  2  0  8  6  4  2  0  8  6  6  8  0  2  4  6  8  0  2  4  6  8  0  2  4
                                                                      X  AT WST3
```

Fig. 17. The predicted beam spot at the WST3 location in the beam line 2A tunnel.

```
                    97/12/29 - 2A AT 500 MEV -- FINAL COORDS + MEASURED Leff - NEW FF

  Space # 5:  Distribution of particles as a function of  X  AT WST4   (Element #106)     (along HORIZONTAL axis)
                                                          & Y  at WST4   (Element #106)     (along VERTICAL axis)

   REAL! Distribution of FINAL RUN FOUND HERE
                                                  COUNTS  = 149986.
                                                    X PROJECTION

                                                                  1  1  1  1  1  1  1
                                    1  2  3  5  7  8  9  0  0  0  0  0  0  0  9  8  7  5  4  2  1
                          1  4  1  2  7  4  1  2  3  0  1  4  3  4  4  1  5  6  3  7  0  5  4  5  1
                          0  6  8  4  9  3  8  4  3  8  2  3  3  7  3  3  3  2  9  2  1  9  0  3  3
                    0  0  1  6  5  0  3  3  4  5  8  1  2  0  8  8  3  3  6  4  5  5  9  4  9  9  5  3  7  0  0
                  +--|--------------|--------------|--------------|--------------|--------------|--------------|+
    0.5800        -                       1                                                                    -       1
    0.5400        |                                          1           1              1                        |       3
    0.5000        |                     1  1  6  5  6  5 10  1 17  6  5  7  7  7  5  6  1  2  2     1           |     101
    0.4600        |                  1  1  9  7 16 29 26 36 26 31 33 35 27 37 26 16 24 17 21 13 11  1     2     |     445
    0.4200        |                  3  5 17 37 46 50 53 55 74 85 76 72 70 79 64 73 61 56 38 22 18 17  2           |    1073
    0.3800        |               1  9 24 36 34 69 87 93118129134139113125129139113107 93 78 50 36 17  8  2     |    1883
    0.3400        |               2 10 24 36 69125149166175209208212202209186206174158144105 65 51 21 12  4     |    2922
    0.3000        |               3 12 37 59120156216205235274271319295261278258239228207156100 75 35 13  3  1  |    4056
    0.2600        |               3 19 38 75145194244314368339350368374360346367321285253177134 80 38 20  5     |    5217
  Y 0.2200        |               5 17 62102176240327355380421433413436462415478382356299241197120 59 26  7     |    6409 Y
    0.1800        -               4 22 61111178279399418496537545531576554551550529432388311209136 65 38  5  1  -    7926
    0.1400        |               8 27 62123232307402471528585545617624660647605577569448313217177 78 29  7     |    8858 P
  A 0.1000        |               5 26 79163239337459529612599613701681665640617624570505373264171 83 31 10  1  |    9597 R
  T 0.6000E-01    |               6 35 94158268404478605679708704749685736728721678634500399265173 83 43 14     |   10547 O
    0.2000E-01    |               6 39 74166275363479626661718714698736707746698699616558404277182 99 28  7  1  |   10577 J
  W -.2000E-01    |            1 10 39 94173257399540607707735683739748767760723715616532436318168112 39 11     |   10929 E
  S -.6000E-01    |               6 36 94135260372494536636762739759759745746777616579530389271205105 40  9     |   10600 C
  T -.1000        |              13 24 71150272382487559623695712680682737716667654605504428296173119 43  8     |   10300 T
  4 -.1400        |               5 35 72154262362457504600653641642669682668676615548487363240168 95 34  6     |    9638 I
    -.1800        |               7 24 64135202333424469529561627627577597641577611502408351282131 89 30  7     |    8805 O
    -.2200        -               6 25 61112214267357436476555525549552548549549467433381295179119 73 27  7  1  -    7763 N
    -.2600        |               4 14 44102159236321381413459473491459430455412420391325259187125 74 25 10  2  |    6671
    -.3000        |               4 14 44 83129187270295325365363374356381365357354316256206140 98 48 17        |    5347
    -.3400        |               4 18 27 51108130190223239271285262280291293268240233209144120 66 27  9  1     |    3989
    -.3800        |               3  4 17 41 63103137159213187188209208208212182177156141105 77 56 33  9  4     |    2892
    -.4200        |               1  8 18 30 41 69 98123111109126127125135137121132107 74 76 47 42 20  8  3     |    1888
    -.4600        |                  3  6 10 27 31 55 59 63 78 66 81 55 70 75 55 62 54 45 34 28  9 12  2        |     980
    -.5000        |                  1  5 10 10 14 25 23 33 23 37 29 28 37 22 29 34 28 27 22 11  5  3     1     |     457
    -.5400        |                     1     2  6  5  8  9  9  5  7  5  2  5  7  7 10  7  3  2  4  2  2        |     108
    -.5800        |                        1     2                                    1                    |       4
    -.6200        -                                                                                          -       0
                  +--|--------------|--------------|--------------|--------------|--------------|--------------|+
                     -  -  -  -  -  -  -  -  -  -  -  -  -  -  -  -  -
                     1  1  1  1  1  1  0  0  0  0  0  0  0  0  0  0  0  0  0  0  0  0  0  0  0  0  1  1  1  1  1
                     .  .  .  .  .  .  .  .  .  .  .  .  .  .  .  .  .  .  .  .  .  .  .  .  .  .  .  .  .  .  .
                     5  4  3  2  1  0  9  8  7  6  5  4  3  2  1  0  0  1  2  3  4  5  6  7  8  9  0  1  2  3  4
                     5  5  5  5  5  5  5  5  5  5  5  5  5  5  5  5  5  5  5  5  5  5  5  5  5  5  5  5  5  5  5
                                                    X  AT WST4
```

Fig. 18. The predicted beam spot at the WST4 location in the beam line 2A tunnel.

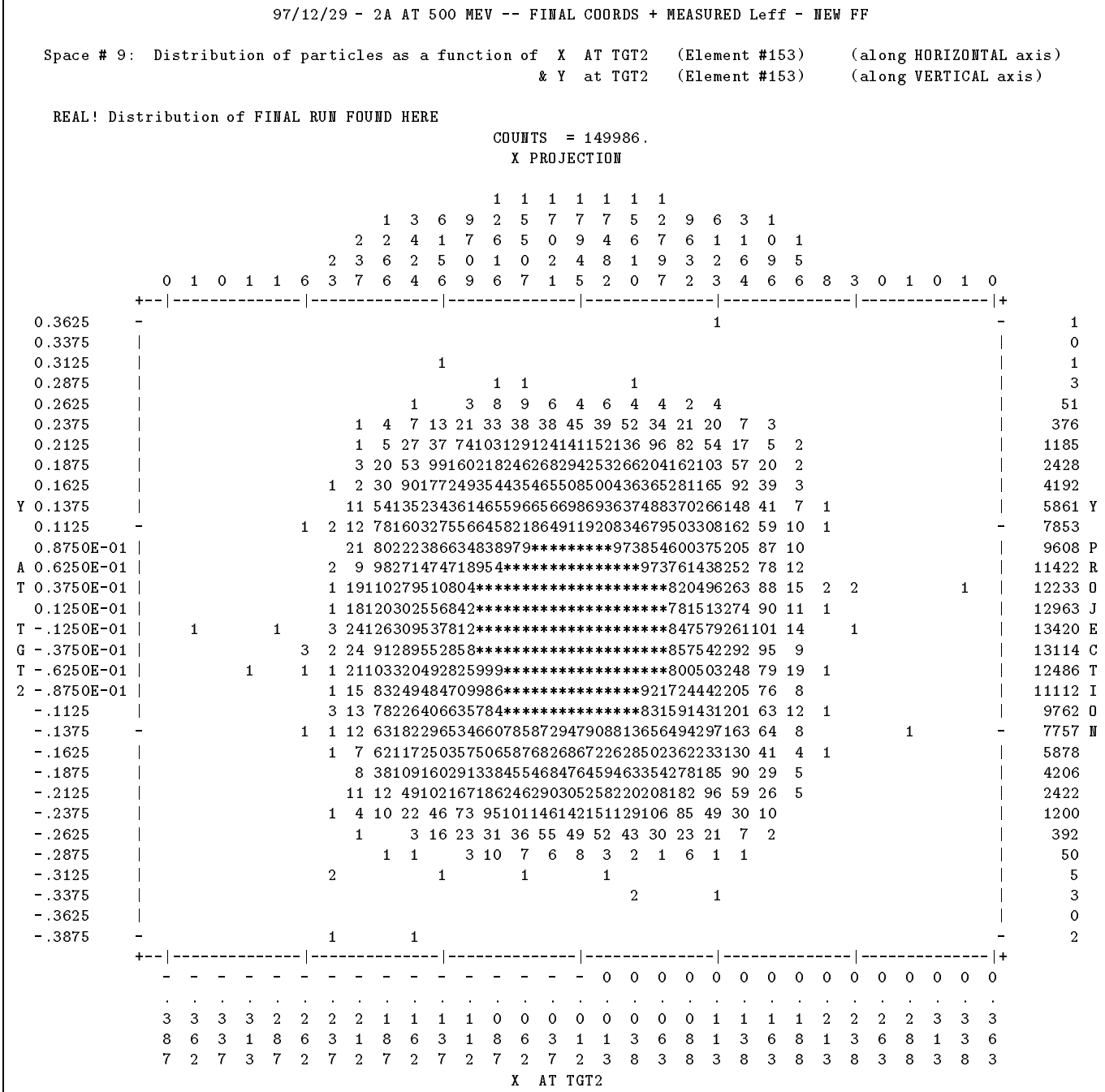

Fig. 19. The predicted beam spot at the west target (TGT2) location of beam line 2A.

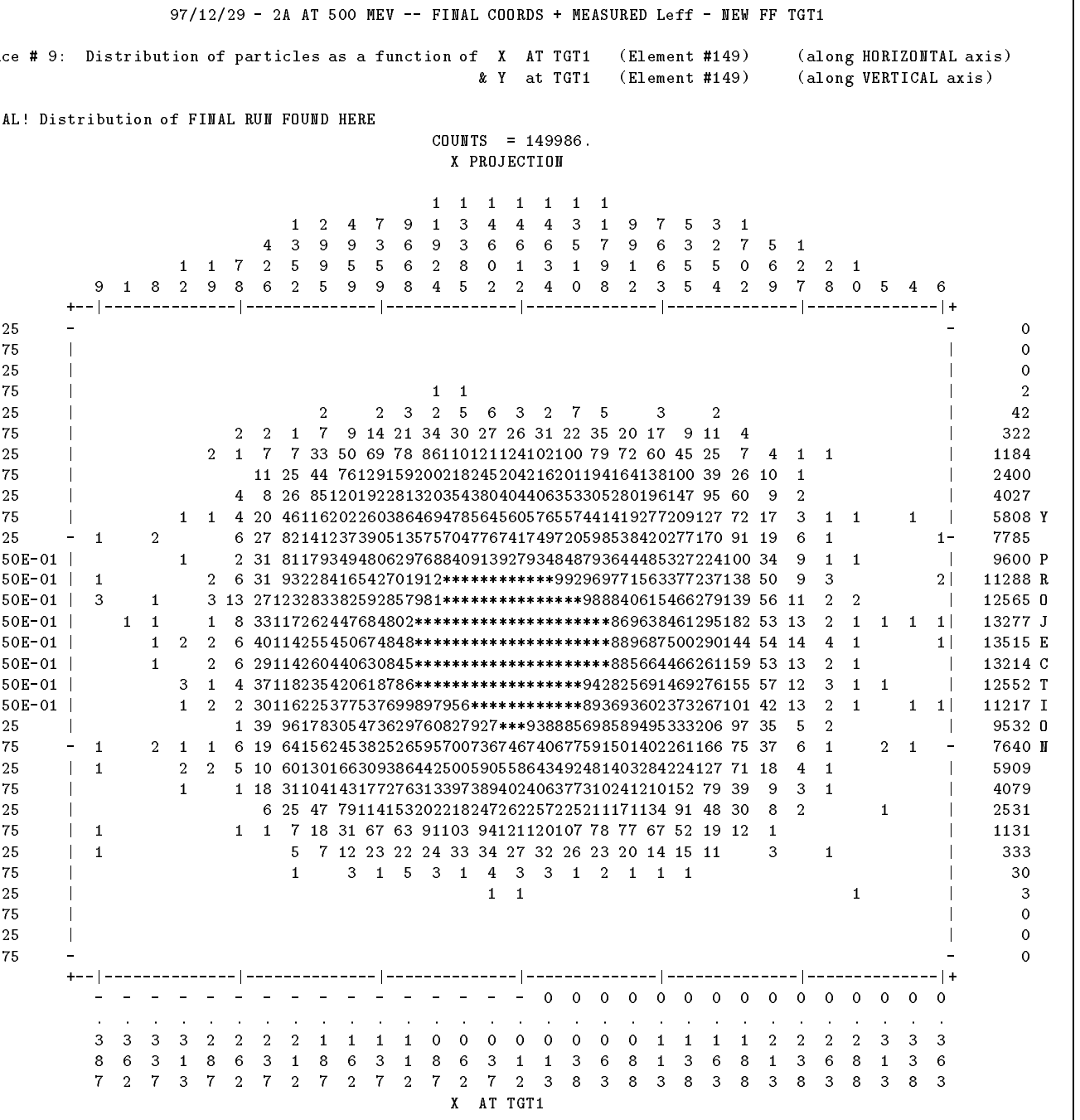

Fig. 20. The predicted beam spot at the east target (TGT1) location of beam line 2A.

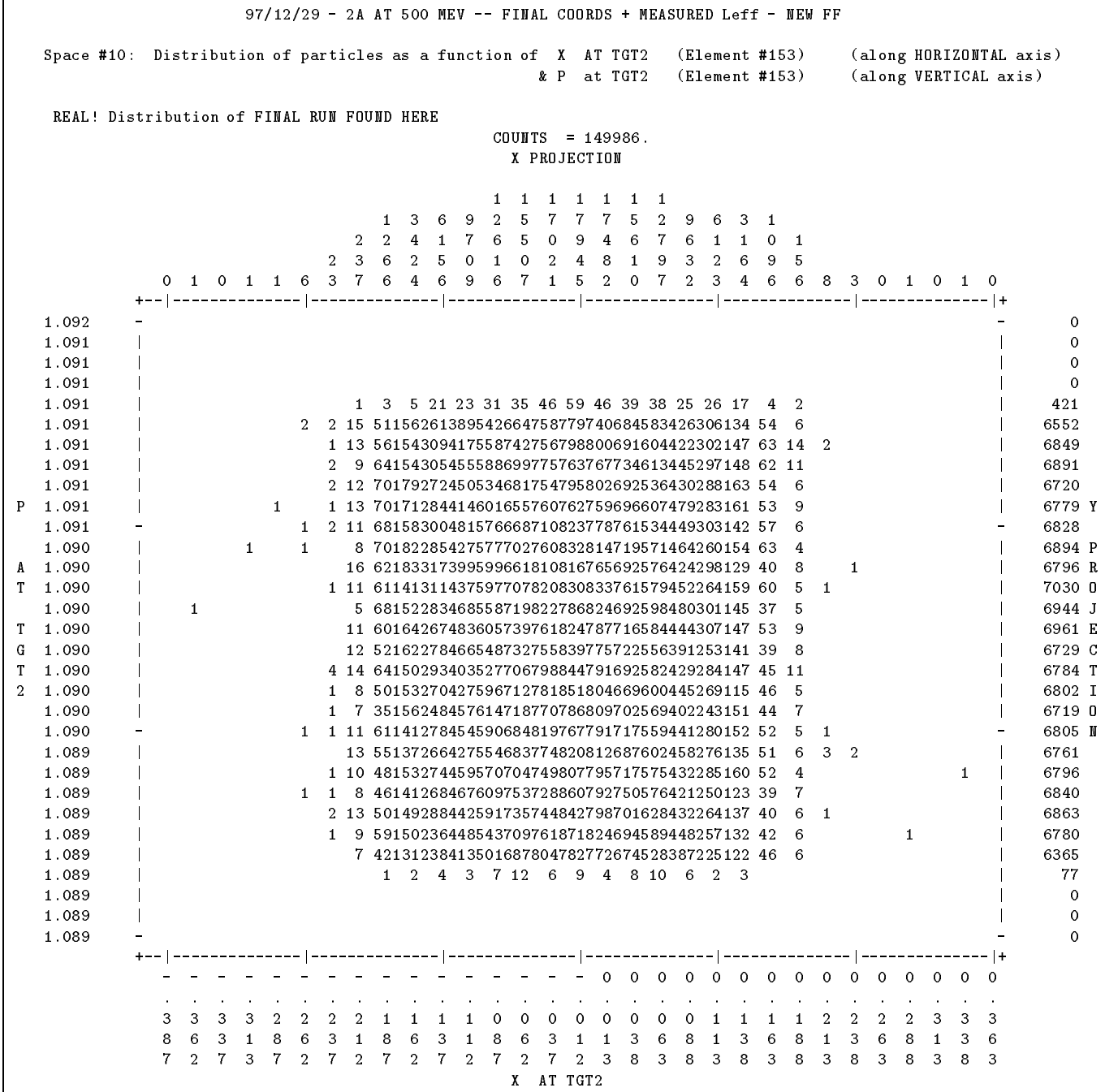

Fig. 21. The predicted momentum-position correlation at the west target (TGT2) location of beam line 2A.

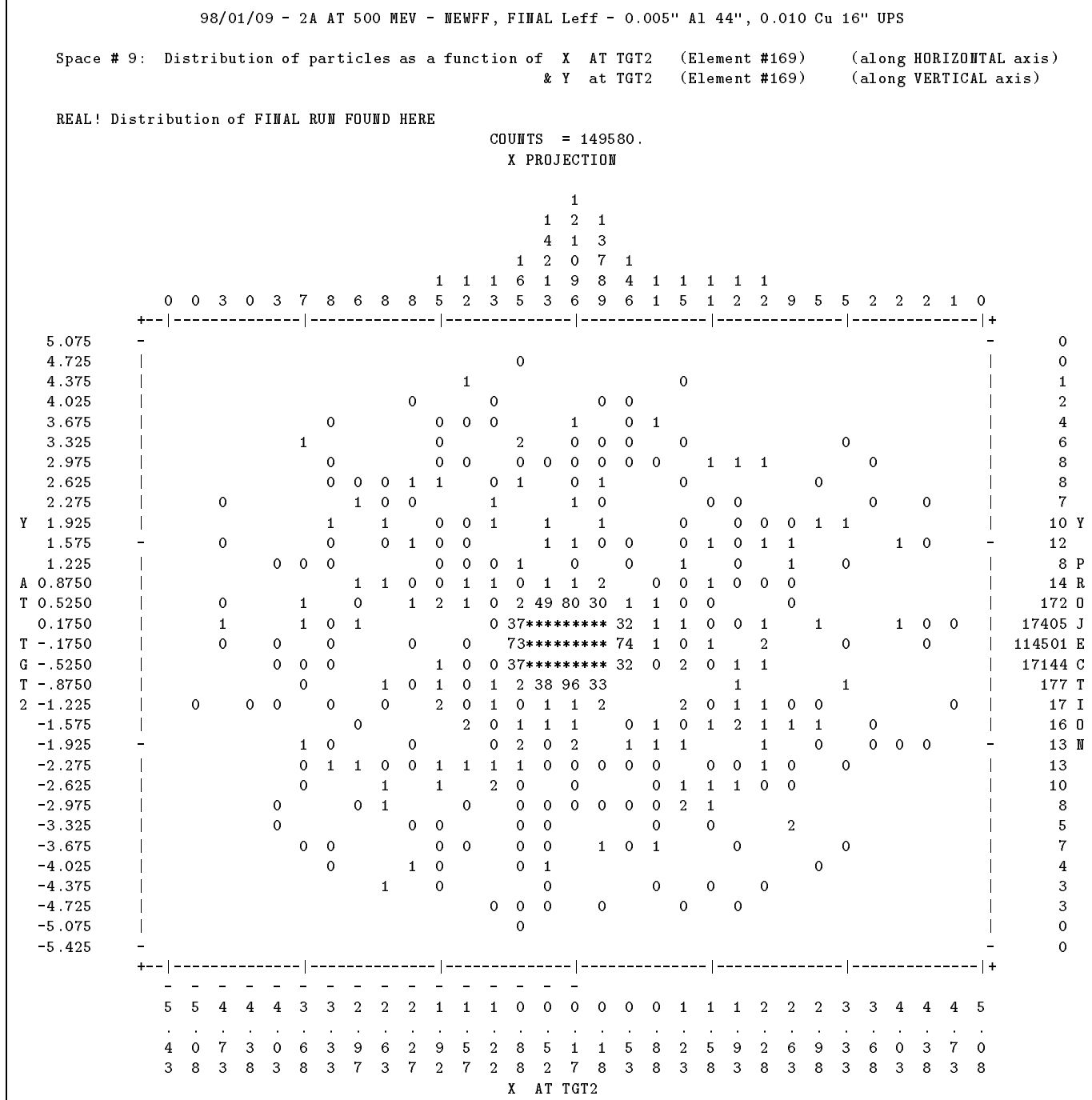

Fig. 22. The effect of the stripper foil and the 0.005 in. Al and 0.010 in. Cu windows on the beam spot at the west target (TGT2) location of beam line 2A.

```
                98/01/09 - 2A AT 500 MEV - NEWFF, FINAL Leff - 0.005" Al 44", 0.010 Cu 16" UPS

  Space # 2:  Distribution of particles as a function of  X  AT TGT2   (Element #169)     (along HORIZONTAL axis)
                                                        & Y  at TGT2   (Element #169)     (along VERTICAL axis)

   REAL! Distribution of FINAL RUN FOUND HERE
                                                        COUNTS  = 149595.
                                                          X PROJECTION

                                                                                1  1  2  2  2  1  1
                                                                             2  5  0  7  4  6  4  7  0  5  2
                                                                          1  1  3  8  1  1  7  8  2  9  0  5  4  1  0  7  3  1
                   8     1  1  2  4  0  8  8  5  8  6  6  4  0  5  2  5  4  1  7  9  1  8  8  4  2           8
                   4  6  0  7  7  2  3  2  0  7  5  4  5  5  2  9  9  9  6  2  2  2  1  3  4  8  3  9  8  2  5
                 +--|--------------|--------------|--------------|--------------|--------------|--------------|+
  0.8700       - 30  1     2  0     1  0     1  1  0  2  1  1  0  3  1  0  1  1  1  2  1  1  1     0  1  0 29-       88
  0.8100       |  1                          0        2                 0                                  1           0|       5
  0.7500       |  1                       0           1  1              1                                  0           1|       6
  0.6900       |  0        0                       2     2        2  3  3  1                                          1|      15
  0.6300       |  0     0                 0  3  2  4  2  1  1  3  5  3  4  2  1  1     1                          0  0  0|      36
  0.5700       |                          2  1  1  2  3  4  4  8  7  7  7  2  1     5  1  1  1                          1|      59
  0.5100       |                          1  4  1  5  5  6 12  9  7 13  1  7  2  7  3  0                             1|      84
  0.4500       |  1                    1  2  3  8  5 15 13 28 16 16 26 19 13 11  9  6  5  5  1  1                    1|     205
  0.3900       |  0     1     1  1  1  3  3  9 12 18 31 47 57 65 74 39 35 36 13  7  9  5  3     2                    1|     474
Y 0.3300       |  0                    2 11 11 24 24 45 871371631901721551105831 14  7  5  7  1  1                 1|    1256 Y
  0.2700       -  1  0        1  1  3  6 14 18 651001973233985004773592411165622 18  6  6  3  1                    1-    2934
  0.2100       |  1     2  1  3  3 10 15 16 37104222490735*********781458236 89 53 22 16  4  1  1  3                 1|    6588 P
A 0.1500       |  0     1     1  5  6 18 26 58185414829**************812350170 63 25 14  5  1     1                 2|   11607 R
T 0.9000E-01   |  0     1  1  2  5  8 13 35 94234601********************569239 81 27 12  5  5  2                    2|   17420 O
  0.3000E-01   |  1  1     2  1  4 12 18 39 95296764********************742275112 31 12 13  4  1                    1|   22158 J
T -.3000E-01   |  0  0     2  3  4  7 18 45107324744********************798285105 33 19 10  2     2  2              |   24045 E
G -.9000E-01   |  1     1  0  2  3 13 17 44116286773********************737270 88 23 11  7  7  2  1              0|   21870 C
T -.1500       |  0     1     4  3 11 16 36108257586********************586231 69 26 27  5  5  5                    1|   17573 T
2 -.2100       |  0  1     1  2  3  6  9 29 74183406785**************818425160 69 39 16  2  5  3     1              0|   11580 I
  -.2700       |  1     1  1  3  2  7 12 24 44 88238462769*********733447220112 43 10 11  4  1  1  1              1|    6435 O
  -.3300       -  0        1     3  7  6 16 24 54123245365442497433331226113 64 25 10  4  3  7  1     2           1-    3004 N
  -.3900       |  1     1  1        4  2  9 17 29 56 72125160180171125 66 68 29 10  8  7  5                       1|    1148
  -.4500       |  1           2  1     5  7  8 11 23 39 52 59 67 70 43 33 25 12  5  6  4  1                       0|     475
  -.5100       |  0        1  1     1  2  8  4  8  9 14 23 16 24 26 22 22  8  9  7  5  4     1                    0|     216
  -.5700       |  0                 2  3  1  3  2  2  9 10  9 10 12 10 13  6  5  2  1                          0  1|     102
  -.6300       |  1        0     1        2     2  6  4  6 12  5  6  4  5  1  2  2  1  1     1                    1|      64
  -.6900       |  1  0     1              2     1  4  1  4  3  1  4  1  1     1                                   1|      26
  -.7500       |                    1           1  1  1     1     2  5  1                                         1|      14
  -.8100       |  1                 1                 2     1  1        1     0                                   1|       8
  -.8700       |  1                          1     1  0     1                                                     0|       5
  -.9300       - 33  2  0  1  1  0  1  2  1  1  1  0  1  2     0  1  0  1  1  0  0  1  1  0  1  1  0  1  0 28-       89
                 +--|--------------|--------------|--------------|--------------|--------------|--------------|+
                    -  -  -  -  -  -  -  -  -  -  -  -  -  -  -  -  -  0  0  0  0  0  0  0  0  0  0  0  0  0  0
                    .  .  .  .  .  .  .  .  .  .  .  .  .  .  .  .  .  .  .  .  .  .  .  .  .  .  .  .  .  .  .
                    9  8  8  7  6  6  5  5  4  3  3  2  2  1  0  0  0  0  1  2  2  3  3  4  5  5  6  6  7  8  8
                    3  7  1  5  9  3  7  1  5  9  3  7  1  5  9  3  3  9  5  1  7  3  9  5  1  7  3  9  5  1  7
                                                        X  AT TGT2
```

Fig. 23. The effect of the stripper foil and the 0.005 in. Al and 0.010 in. Cu windows on the beam spot at the west target (TGT2) location of beam line 2A.